# CONTAMINATION RISK AND GEOPHYSICAL SIGNATURE OF ABANDONED WELLS IN THE GULF COAST AQUIFER SYSTEM, TEXAS

A Thesis

by

TEJASWINI PENCHALA

B.Tech., Vaagdevi College of Engineering - India, 2018

Submitted in Partial Fulfillment of the Requirements for the Degree of

MASTER OF SCIENCE

in

ENVIRONMENTAL SCIENCE

Texas A&M University-Corpus Christi
Corpus Christi, Texas

December 2021

© Tejaswini Penchala

All Rights Reserved

December 2021

CONTAMINATION RISK AND GEOPHYSICAL SIGNATURE OF ABANDONED WELLS IN THE GULF COAST AQUIFER SYSTEM, TEXAS

A Thesis

by

TEJSWINI PENCHALA

This thesis meets the standards for scope and quality of
Texas A&M University-Corpus Christi and is hereby approved.

Ahmed Mohamed, PhD
Chair

Dorina Murgulut, PhD
Committee Member

Jennifer Smith-Engle, PhD
Committee Member

December 2021

ABSTRACT

Over the years, many oil and gas wells have been abandoned, without proper plugging, around homes, farms, industrial sites, and urban areas. These abandoned wells are potentially becoming pathways for groundwater contamination through short-circuiting between aquifer units. The primary goal of this research is to create a risk map for the Texas Gulf Coast Aquifer (GCA, area: 108 x $10^3$ $km^2$) showing locations that are prone to groundwater contamination due to the presence of abandoned oil and gas wells. For this purpose, a Generalized Linear Regression model (GLR) was constructed and calibrated using the Geographic Information Systems (GIS) environment. Model inputs included well locations, surface lithology, locations of petroleum storage tanks, superfund points, wastewater outfalls, landfill sites, surface reservoirs, slope, stream density, and rainfall rates. Some of the abandoned wells might be buried underground over the years, identifying these wells is important to plug and eliminate their risk of contamination. To help identifying the buried wells, different geophysical datasets (magnetic, electromagnetic) were acquired and processed to explore their geophysical signature. The geophysical data was collected at the TAMU-CC's geophysical test site, where multiple well covers and steel drums were installed at various depths. Modelling results indicated that 11.53% of the total area of the GCA region is under high risk of groundwater contamination, whereas 43.79% of the area is at moderate risk, 31.05% of the area is at low risk, and 13.61% of the area is at no risk. The high-risk zones are mostly concentrated in the central part of the GCA region (Liberty, Jefferson, Jackson, Live Oak, Zapata, Washington, Calhoun, Chamber, and McMullen counties) and the risk-free zones in the southern part (Duval, Jim Hogg, Webb, Kenedy, Brooks, Lavaca, and Polk counties). Geophysical investigations indicated that both magnetic and electromagnetic anomalies were mainly generated, and correlated with the locations of, the buried drums (45,450–45,700 nT for magnetic, 226–254 mS/m for electromagnetic). Relatively lower magnetic and electromagnetic anomalies are associated with the locations of the well covers (45,200–45,400 nT for magnetic, 210 –222 mS/m for electromagnetic). Our research results could be utilized by decision makers to develop enhanced mitigation scenarios for risks associated with abandoned wells in Texas and around the globe.

## ACKNOWLEDGEMENTS

First and foremost, I am extremely grateful to my esteemed advisor, Dr. Mohamed Ahmed for the invaluable advice, continuous support, and patience during my master's study. His immense knowledge and plentiful experience have encouraged me in all the time of my academic research and daily life. I would like to extend my sincere thanks to my graduate committee members Dr. Dorina Murgulet and Dr. Jennifer Smith-Engle for their technical support and expert inputs which made my thesis more impactful. I will be forever grateful for the help provided by my committee members.

I would also like to thank my colleagues of the Geophysics lab (Michael Haley, Amanda Beattie, Samantha Shyrigh, Dionel Colmenero, Ryan Turner, and Lilia Zavala) for their kind help and support that have made my study and life in the Texas A&M University a wonderful time.

TABLE OF CONTENTS

LIST OF FIGURES

LIST OF TABLES

Page

# CHAPTER I

# Introduction

## 1. Background and Relevance

According to the Texas Railroad Commission (RRC), there are 176,879 active oil wells and 88,240 active gas wells in Texas as of April 2019 and 43% of the nation's crude oil production was from Texas in 2020 (Nicot 2008). When these wells are out of their productive life, or they fail to reach their productive economic quantity, they are plugged and abandoned to avoid any leaks. But some operators leave the wells orphaned without plugging (Hillebrand and Fish 2018). These abandoned wells are a potential threat to the environment as they act as the gateways for the transportation of the surface contaminants into the aquifers through surface infiltration and between aquifers. RRC reported that there are 6,328 orphaned wells in Texas which are inactive for more than 12 months. Abandoned wells are frequently left unplugged, but even plugged wells might leak if they are plugged with less durable materials or if they were plugged in the past when plugging processes were less effective (King 2012; King and Valencia 2014). These unplugged or poorly plugged wells may contaminate groundwater and the surface environment (Anderson et al. 2013). Figure 1 shows the potential for groundwater contamination due to abandoned wells.

Old, unplugged wells, or those with defective well casings or cement, can allow oil, gas, or saline water to flow into freshwater aquifers, and are referred to as orphaned/abandoned wells in this study. An analysis of 185 cases of groundwater pollution in Ohio between 1983 and 2007 identified 41 cases of orphaned well leaking, compared to 113 cases of drilling and production (Reforms 2011).

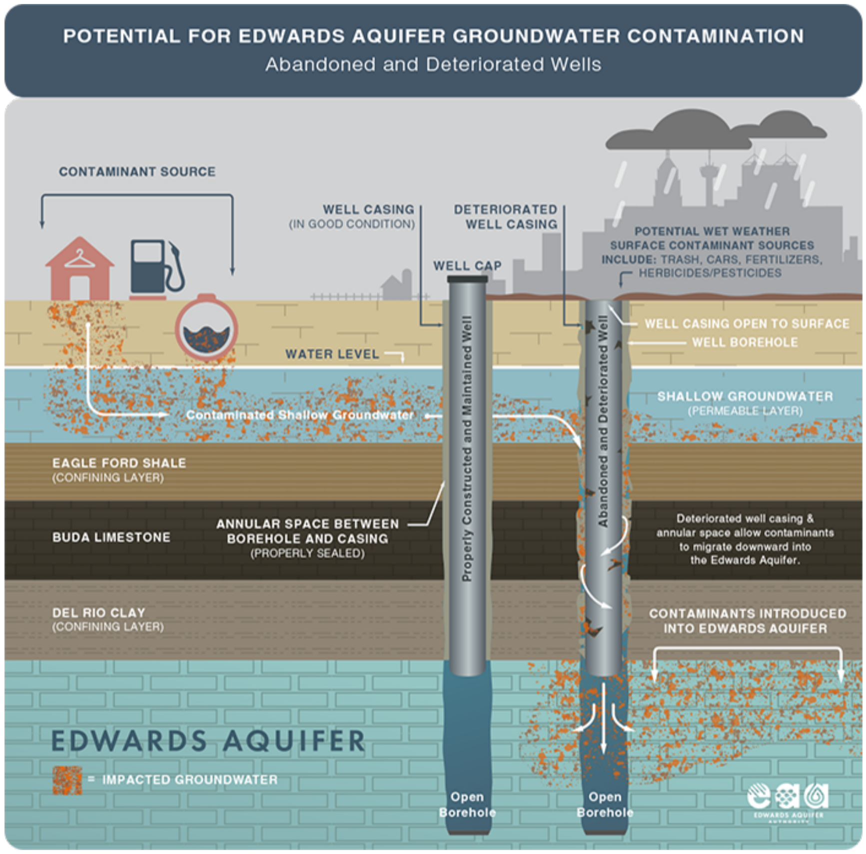


Figure 1 Schematic diagram showing aquifer contamination due to abandoned wells (Edwards Aquifer Authority 2019)

Surface contamination from tiny spills, outdated equipment, and other debris may still exist at abandoned well sites. Gas, oil, salty water, or drilling mud can rise up the well and spill onto the ground surface in some improperly or unplugged wells (Davies et al. 2014). Many wells have been left unplugged in many areas, such as in Pennsylvania, California, and Texas, where drilling began prior to the turn of the 20th century. The plugging method of abandoned wells was much less adequate than it is today (Vrålstad et al. 2019). If these plugged wells are allowed to leak, these leaks can travel to the Earth's crust where gas, oil, and formation waters saturate the topsoil and surface expressions can form. Mapping areas that are susceptible to risks from contamination due to the presence of abandoned wells is essential for sustainable management plans and a cleaner water resource. In this research, a risk map for abandoned wells was generated for in the Gulf Coast Aquifer (GCA) of Texas.

From 1984 to 2008, the RRC plugged almost 35,000 orphaned wells, at the cost of over \$163 million. The RRC plugged 918 orphaned wells at the cost of over \$11.6 million in the fiscal year 2017. There were roughly 10,000 abandoned wells in Texas that required plugging, as of December 2017; RRC plugged 1,477, 1,364, 1,710, and 1,477 abandoned wells as in 2018, 2019, and 2020 respectively (RRC 2021a). Decision makers usually mitigate the risks of abandoned wells by plugging them. Although the latitude and longitude information are available for those wells, locating them in the field would be challenging and time-consuming task especially if they are buried underground. Geophysical investigations provide a robust approach to locate those abandoned wells. Identifying the geophysical signatures of the buried abandoned wells will enable efficient and cost-reduced mitigation scenarios. In this research, we investigated the magnetic and electromagnetic geophysical response of abandoned wells.

## 2. Objectives

The purpose of this research is to develop a risk map for the GCA, showing areas that are more susceptible to contamination by the abandoned wells. To do that, we constructed and calibrated a weighted overlay model to estimate the risk of GCA contamination. Factors affecting the risks from abandoned wells were used as model inputs.

We also acquired and processed different geophysical datasets (magnetic, electromagnetic) to explore the geophysical signature of the buried abandoned wells. This study can be used to locate the buried abandoned wells. The geophysical data were collected at the Texas A&M

University-Corpus Christi (TAMUCC)'s geophysical test site, where multiple-well covers, drums were installed at various depths.

## 3. Study Area

### a. Gulf Coast Aquifer (GCA):

The GCA system is the largest aquifer system in the Texas, and it is the main source of groundwater for the state (Figure 2).

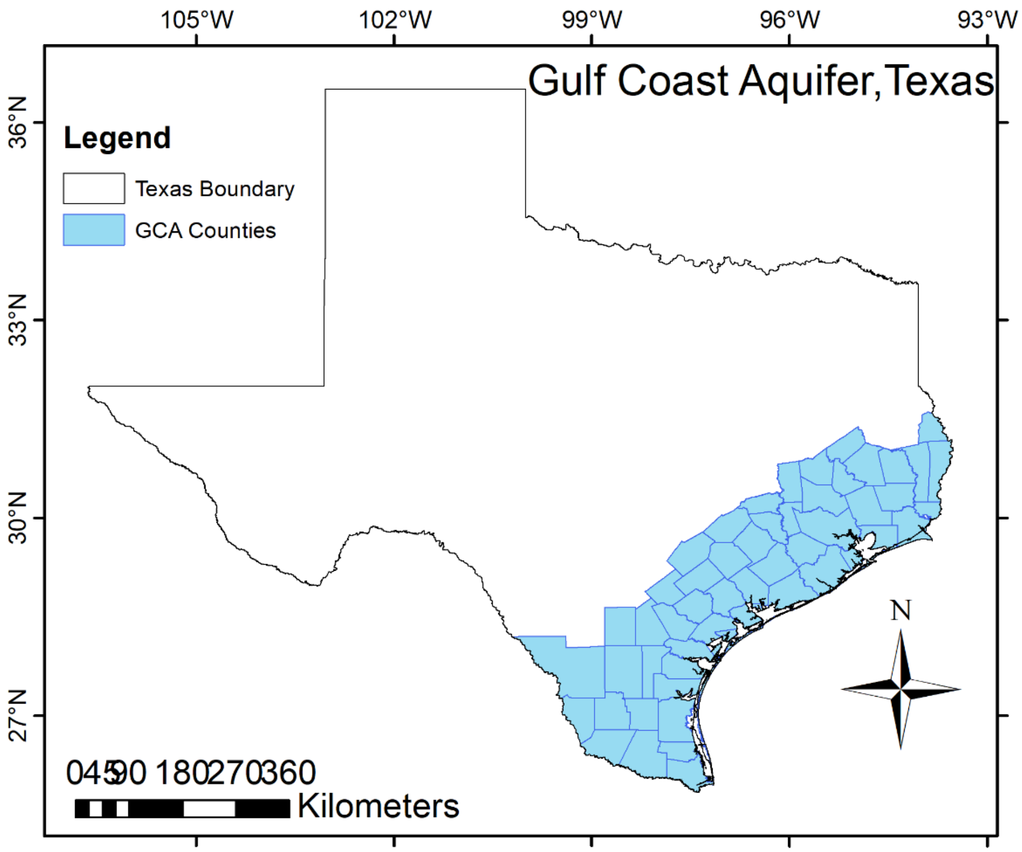


Figure 2 The spatial distribution of the GCA in Texas.

It runs long the of the Gulf of Mexico coast, covering all or portions of 56 counties. The Evangeline, Jasper, and Chicot aquifers, for example, are made up of discontinuous clay, sand, gravel, and silt beds, and make up the GCA system. The GCA has a maximum total sand thickness of 1,300 feet in the north and 700 feet in the south. The average thickness of saturated waters is about 1,000 feet (Mace et al. 2006).

The quality of the water varies depending on its depth and location. To the south, as the aquifer's productivity drops, it becomes more saline, with total dissolved solids (TDS) ranging from 1,000 to more than 10,000 milligrams per liter. In contrast, in the central and northeastern parts of the aquifer the water quality is good with TDS less than 500 milligrams per liter. Saltwater intrusion in reaction to brine migration, groundwater pumping, oil field operations, and natural flows from salt domes intruding into the aquifer may be linked to areas of increased salinity throughout the central and eastern Gulf Coast. Irrigation, municipal, and industrial reasons are all served by the GCA. Water level drops of up to 350 feet have caused ground subsidence in Harris, Jasper, Galveston, Fort Bend, and Wharton counties (Mace et al. 2006). Throughout the GCA, high levels of alpha radiation are found. The northern GCA has the greatest combined radium concentrations (radium-226 and radium-228) and southern GCA has the uranium exceedances (Reedy et al. 2011).

Because of the cyclic deposition of sedimentary facies, the geology of the GCA is complicated. The GCA sediments were mostly deposited in the Gulf of Mexico Basin's coastal lowlands. These sediments were deposited in fluvial-deltaic to shallow-marine environments from the Miocene to Pleistocene periods. Discontinuous strata of clay, gravel, silt, and sand resulted from natural basin subsidence and recurrent sea-level shifts. Six primary sediment dispersal systems originating from massive deltas distributed sediments from the Laramide Uplift erosion along the southern and Central Rockies, as well as the Sierra Madre Oriental. (Galloway et al. 2000).

The GCA is mostly covered by a smooth, low-lying coastal plain that rises gradually from sea level in the east to up to 900 feet in the west and north. The coastal uplands come to an end at the Cretaceous clay and limestone contact, where altitudes rise rapidly. The surface geology of the Texas Gulf Coast is complicated, with a mosaic of lithofacies spanning most of the outcrop regions, including Holocene and Pleistocene sediments. The Coastal Plain is buried behind a thick layer of sediments that forms a homocline descending progressively towards the Gulf of Mexico. Texas has a history of oil/gas production of more than 100 years, being the leading crude oil producer in the nation. The oil and gas extraction is comparatively  more within the GCA region, apart from the Permian Basin (Banga et al. 2011). The total oil and gas extracted in Texas is 4,841,205,399 barrel of crude oil (BBL)/year out of which 73,971,641 BBL/year is extracted over the GCA region(RRC 2021b). The average depth of an oil/gas well in the GCA is 6,000 feet (Nicot 2008).

**b. Geophysics Test Site (GTS):**

The GTS was constructed at the Texas A&M University-Corpus Christi by Dr. Mohamed Ahmed and the geophysical lab to study different geophysical techniques and to better the teaching and research opportunities (Ahmed et al. 2021). The GTS serves as an opportunity to learn different geophysical techniques and their practical responses to known objects. Figure 4 shows the location of the GTS in Texas. The GTS is a 50m x 50 m (2,500 $m^2$) area located at the Thomas J Henry Tennis Center of Texas A&M University-Corpus Christi (Ahmed et al. 2021). Subsurface targets of different materials such as well covers, plastic drums, steel pipes, steel drums were buried at different depths ranging from 0.5m to 3m to explore their geophysical signatures (Figure 3). This selection of subsurface targets was based on magnetic, electric, and electromagnetic responses. This test site served as a real-world example of a contaminated site that might contain drums apart from well covers in this research.

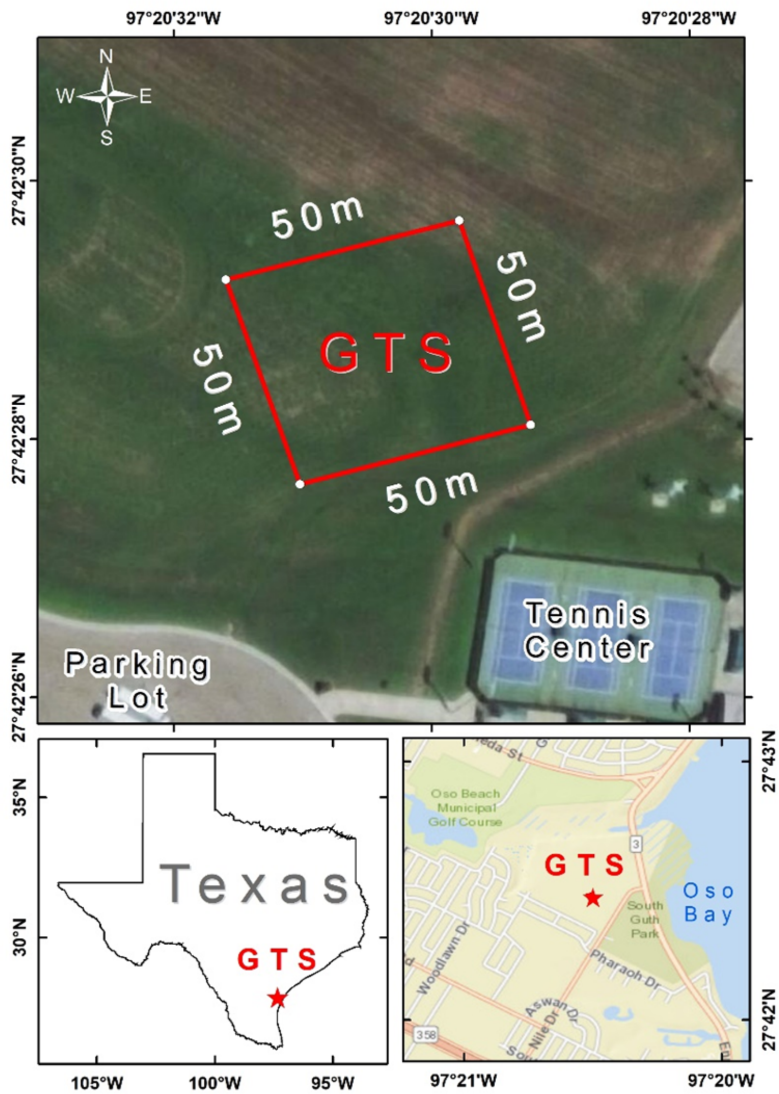


Figure 3 Location map showing the 50 m × 50 m GTS location (top). Also shown is the GTS regional location in Texas (bottom left) and Corpus Christi (bottom right).

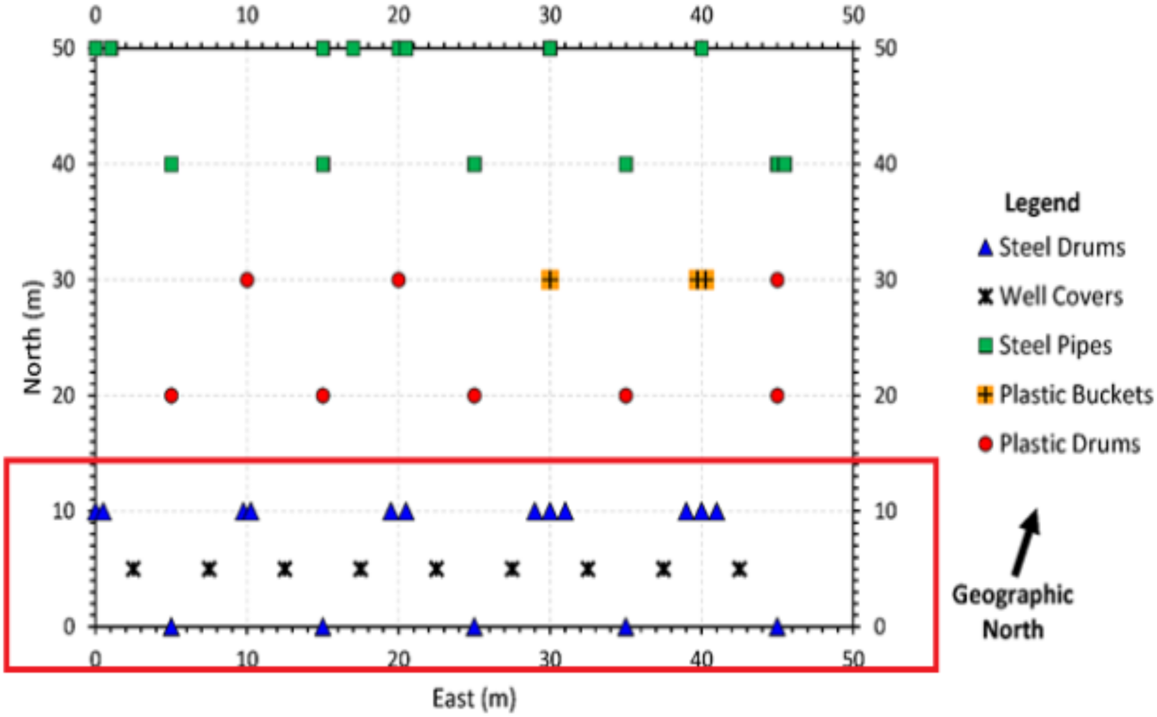


Figure 4 Subsurface targets at GTS. The red rectangle shows the locations of the well covers.

# CHAPTER II

## Data and Methods

### 1. Risk Map of GCA

In this research, we used a data-driven statistical approach, a Generalized Linear Regression (GLR) model, to create a risk map for the GCA. This model has been also used in mapping landslide susceptibility mapping (Khodadad and Jang 2015), analysis of particulate air pollution in Hamilton (Jerrett et al. 2016), and modeling of Covid-19 incidence rate in continental United States (Mollalo et al. 2019).

Three major steps were conducted to generate this risk map. The first step was to determine the model input layers, the second step was to process the dataset of each input layer, and the last step was to generalize the model results over the entire GCA system.

#### a. Input Criteria for Risk Mapping

Over the entire GCA, model input layers include abandoned wells, rainfall, slope, surface lithology, stream network, geologic structures, surface reservoirs, wastewater outfalls, landfill points, superfund points, and petroleum storage tanks. These inputs layers were selected based upon their contribution towards the acceleration or deceleration of pollution in the GCA due to abandoned wells.

***Abandoned Wells:***

Regions with high well density are more vulnerable to groundwater contamination (Nellis et al. 1998; Hussein et al. 2019). We acquired datasets on abandoned wells that were orphaned for more than twelve months as of August 2020. Dataset was acquired for locations of abandoned wells, their operators, counties in which they are located, and the API numbers of wells from RRC.

Abandoned wells are unevenly distributed throughout the GCA region (Figure 5). The concentration of wells is higher in the middle and southern parts of the region compared to the northern part.

A buffer distance was calculated for each abandoned well using the Euclidean Distance tool in ArcGIS platform which gives the distance from each cell in the raster to the closest source based on the straight-line distance from cell center to cell center. This calculated distance helps us to classify the layers based upon the density (the closer the sources, the higher will be the density, therefore the higher chance of contamination and vice versa).

***Superfund Points:***

Superfund sites require a long-term response to clean up hazardous material contaminations and are a source of surface and underground contamination (Callahan et al. 1991). They also aid in increasing the contamination of the aquifer apart from surface contamination (Haley et al. 1989). The dataset of superfund points in the GCA region was acquired from the Texas Commission of Environmental Quality (TCEQ). The data show that there are 72 superfund sites in the GCA region, and they are mostly concentrated in Victoria and Calhoun counties as it is dominantly an industrial area and there are only a few locations in the rest of the region closer to the coast (Figure 6). The dataset was processed and reclassified using the Euclidean distance tool as described in the previous (abandoned wells) section of this paper.

***Wastewater Outfalls:***

Wastewater outfalls or sewage outfalls are a direct source of water pollution. Though the wastewater that are released at the wastewater outfall points are treated, there are cases that prove that they are still a source of pollution (Palmer and Menninger 2013). Just as the abandoned wells

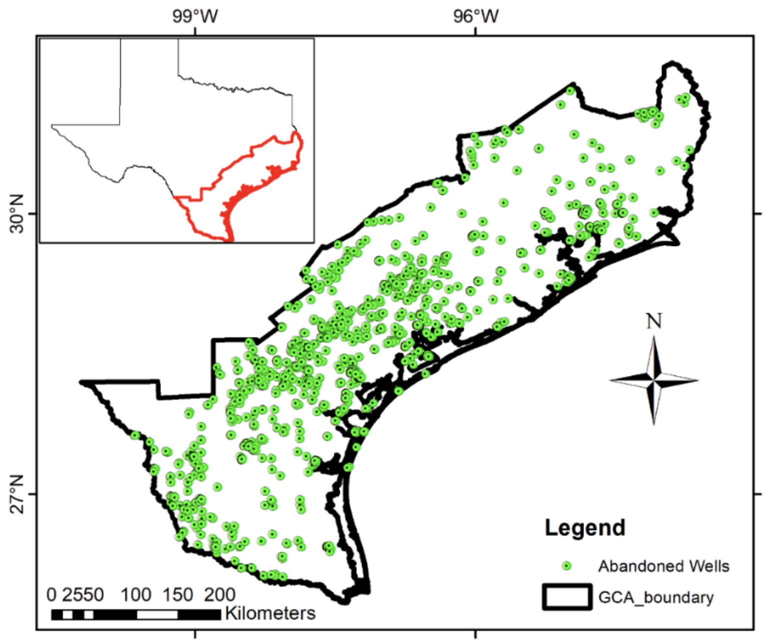


Figure 5 Spatial distribution of abandoned wells in the GCA system.

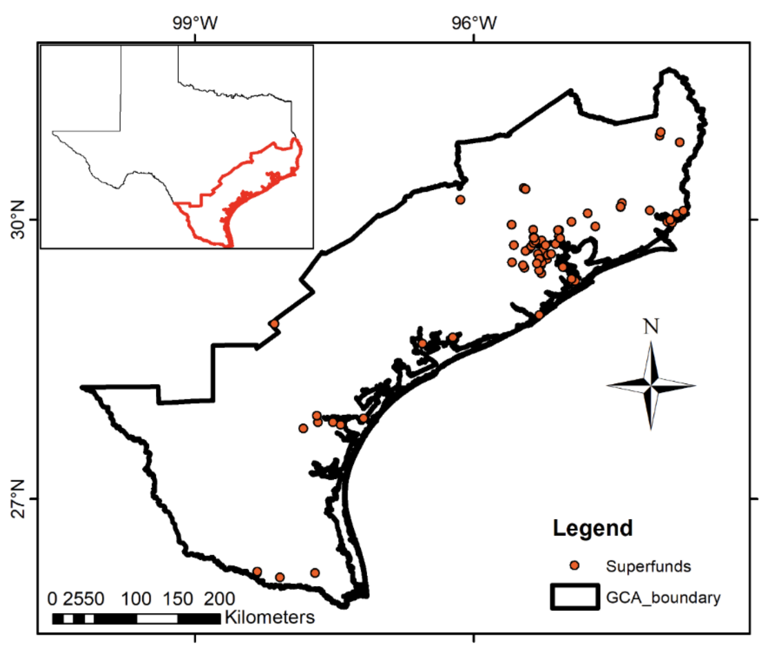


Figure 6 Spatial distribution of Superfund points in the GCA system.

act as gateways for the surface pollutants to contaminate the groundwater, the wastewater outfall points can be considered potential sources of groundwater contamination (Barilari et al. 2020). Surface runoffs and/or floods can carry surface contaminants from these sources towards abandoned wells. Data on the wastewater outfalls in the GCA region were collected from the TCEQ which shows that there are 2,212 locations of wastewater outfalls over the GCA region (Figure 7). The data collected from the TCEQ were processed and reclassified using the Euclidean distance tool as described previously. These sites are high in number hence the higher risk of contamination.

***Landfill Sites:***

Landfill points are a direct source of ground pollution. Leachates formed due to the water that percolates from a landfill site causes pollution when carried into the waterbodies (Rana et al. 2018). Cases of groundwater pollution from leachates prove that the landfill sites near an abandoned well can be an important source of groundwater pollution as the contamination will be highly accelerated (Rana et al. 2018). Data on the landfill sites over the GCA region were collected from the TCEQ (Figure 8) and were processed using the Euclidean distance tool as described in the abandoned wells section.

***Petroleum Storage Tanks:***

Both underground and aboveground petroleum storage tanks are considered to be harmful to the environment as they hold toxic material such as waste oil and gasoline (Sierraclub 2004). Leaks or spills from a petroleum storage tank can directly cause groundwater pollution and the presence of abandoned wells will only increase the rate and pace of contamination (Teng et al. 2013). Data collected from the TCEQ, shows that there are a total of 6,926 petroleum storage tanks

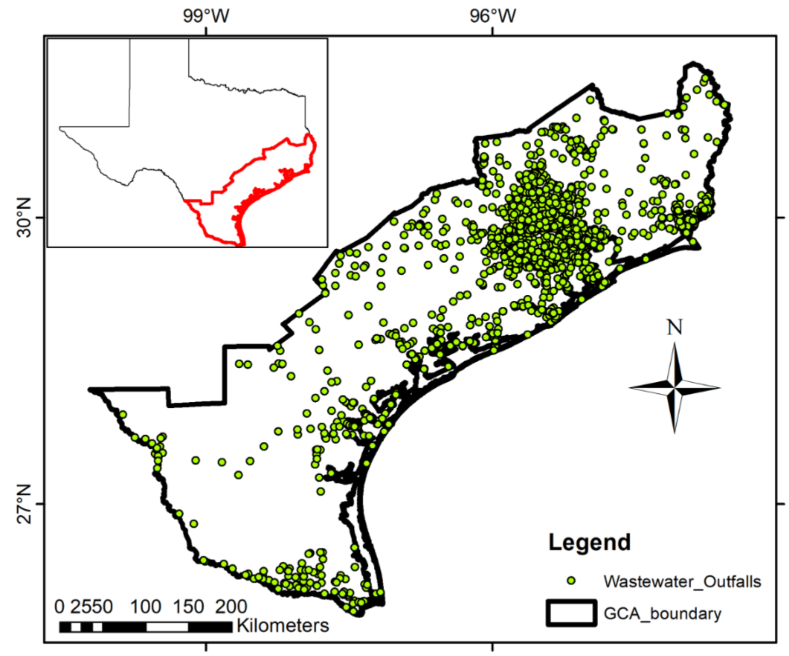


Figure 7 Spatial distribution of Wastewater outfalls in the GCA system.

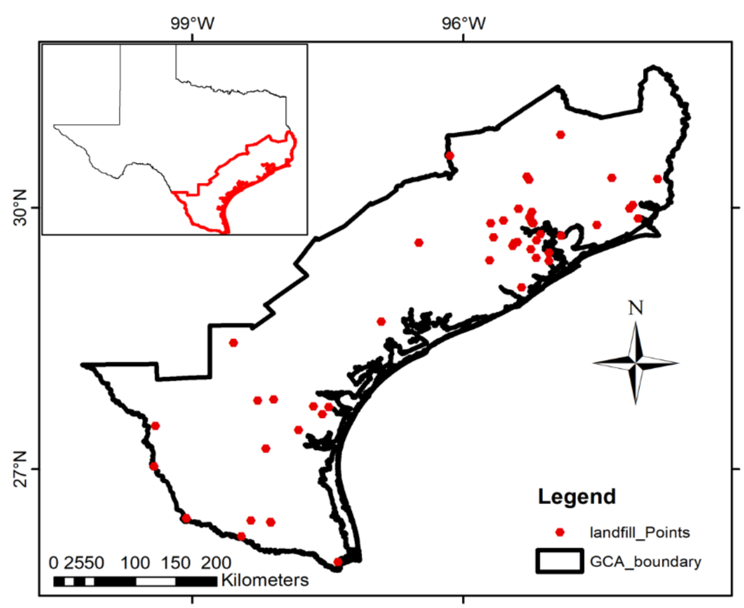


Figure 8 Spatial distribution of landfill points in the GCA system.

in the GCA region. with most located in the northeastern and southern parts of the GCA region. In addition, they are higher in number compared to the other data of this section such as superfund and landfill sites (Figure 9). These data were processed using Euclidean distance tool as described in the abandoned wells section.

***Stream Networks:***

Flowing water carries surface pollutants to the underground through the abandoned wells (Harris et al. 1996). Rivers and streams not only aid travel of the pollutants to the groundwater but also cause corrosion of the metal walls of the well and cause cracks to the cement walls which enhances the contamination by retaining soil moisture (Abdalla and Shamrukh 2016). Stream network data from the Texas Water Development Board (TWDB) was reclassified similar to the abandoned wells given that of the higher presence of streams, the greater the risk of groundwater pollution. There are seven major rivers flowing through the GCA region with streams distributed evenly throughout the region except for the southern part where the stream network is sparser (Figure 10). Distance to streams was classified using the Euclidean distance tool as in the case of abandoned wells.

***Precipitation:***

High precipitation causes runoffs to carry surface contaminants underground through abandoned wells, polluting the groundwater (Zaporozec 1981). Precipitation also percolates into the ground and corrodes the walls of the well, aiding in pollution of the aquifer by leaking the contaminants from within the well (Pátzay et al. 2003). Precipitation data acquired from TWDB was reclassified according to the amount of rainfall. The highest rainfall contributes more to contamination and vice versa. The precipitation is highest in the north and gradually decreases

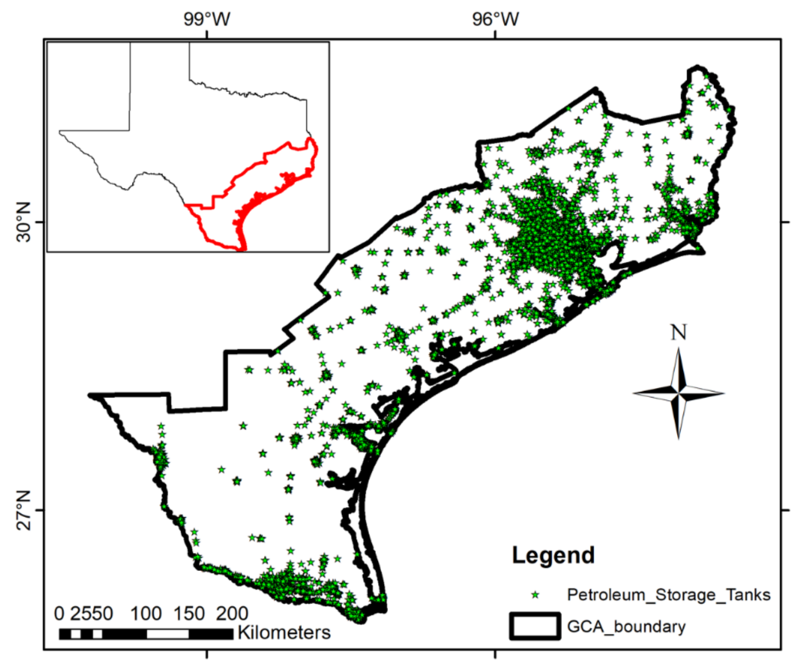


Figure 9. Spatial distribution of petroleum storage tanks in the GCA system.

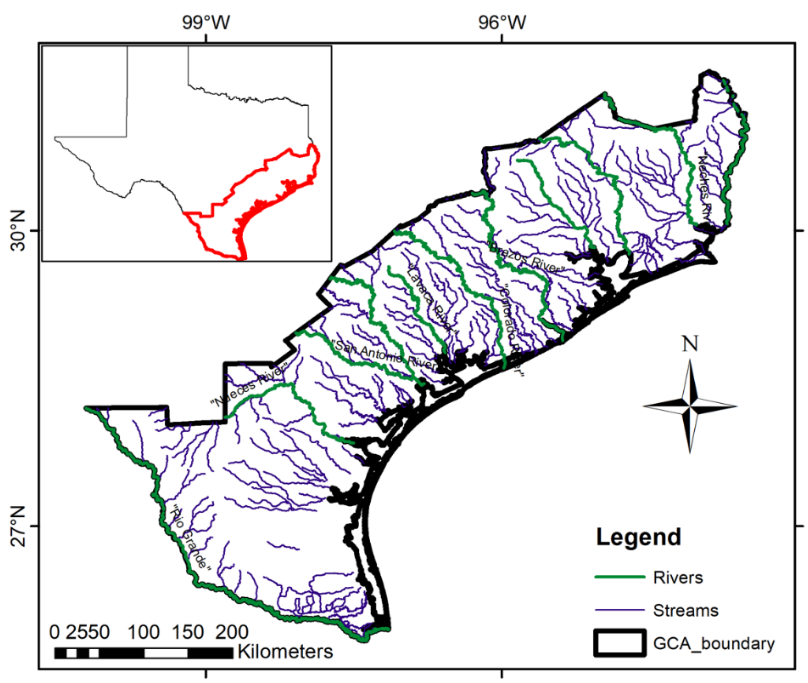


Figure 10 Spatial distribution of rivers and streams in the GCA system

towards the south. According to the data the highest recorded precipitation is 1549.4 mm, and the lowest recorded precipitation is 457.2 mm (Figure 11).

***Surface Reservoirs:***

Regions with more reservoirs is more vulnerable to flooding (Acreman 2000). Floods carry surface contaminants into the wells that lead them to the aquifer and often carry the oil, gas, and other pollutants to the Earth's surface that result in surface pollution in water and soil (Davies et al. 2014). The data of existing reservoirs obtained from the TWDB, were reclassified as done with the abandoned wells data.

The reservoirs in the GCA system are Toledo Bend, Steinhagen, Livingston, Lake Paula, Gibbons Creek, Lake Houston Sheldon, Dutton Lake, Smithers Lake, Mustang Lake, Harris, Brazoria, Eagle, Cedar Creek, Evaporation, Cooling Water, Lake Gonzales, Coleto Creek Cooling Pond, Yarbrough Lake, Barney M Davis, Delta Lake 1, Valley Aores, Loma Alta, Falcon, and Lake Casa Blanca from north to south respectively (Figure 12).

***Lithology:***

Surface and subsurface lithological data were acquired from TWDB as geology plays a major role in horizontal and vertical transportation of the contaminants to the aquifers and between different aquifer units (Maxwell and Kastenberg 1999). In multi-aquifer systems, permeable soils such as sand and gravel may provide paths for contaminants to travel from the abandoned wells into the aquifers and also transport the contaminated water from one aquifer to another aquifer (LeGrand 1964; Talabi and Kayode 2019). Different land conditions play different roles in carrying or obstructing the particles, so the data were reclassified based on their role in aiding

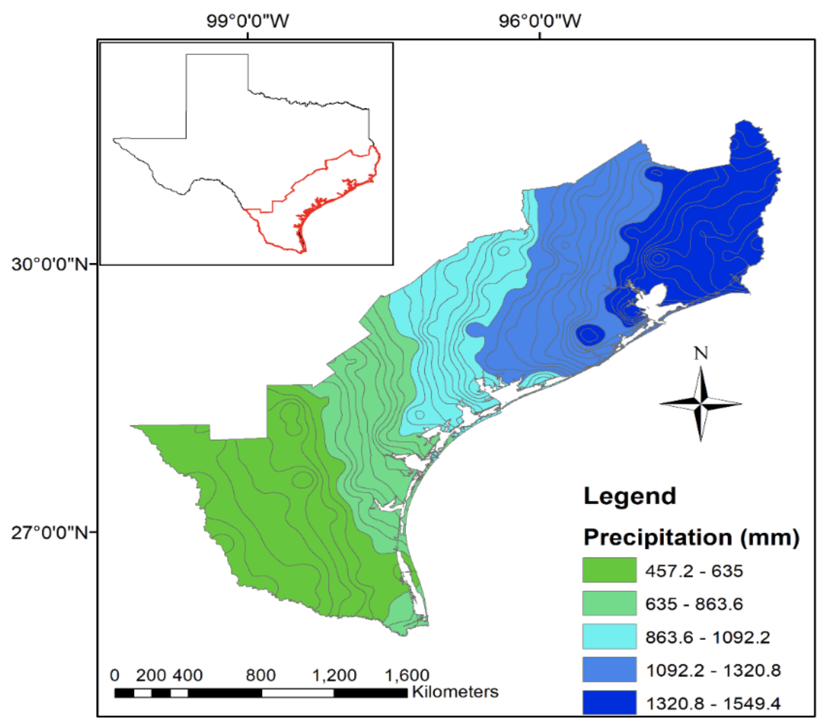


Figure 11 Precipitation over the GCA system.

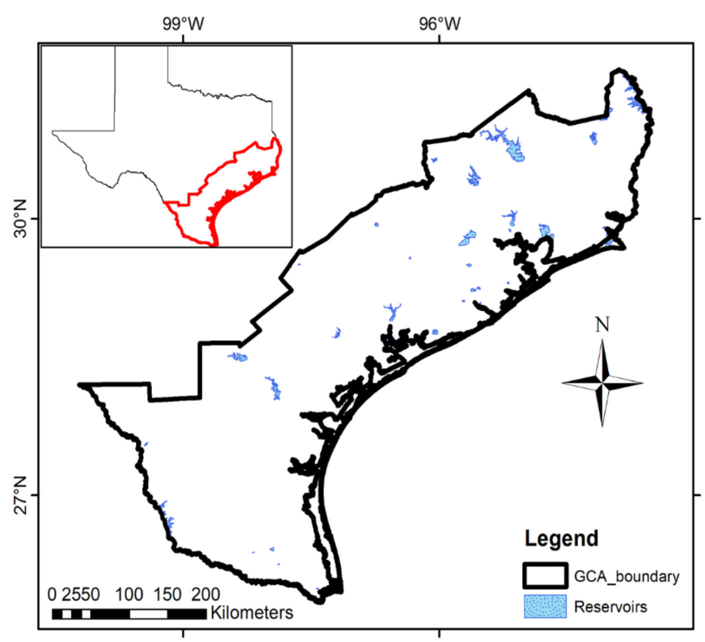


Figure 12 Spatial distribution of reservoirs in the GCA system.

contamination. About 40%of the Gulf Coast region consists of clay, mud or silt and nearly 40%of land which is closer to the coast is sand or water (Figure 13). The rest of the ground consists of different soil types including mudstone, sandstone, gravel, clastic, terrace, siltstone, and indeterminate materials. The lithology layer was divided into seven different layers (one layer for each soil type: Clay/mud, sand, gravel, water, siltstone, terrace, and silt) and these layers were reclassified by assigning a value of 1 for the soil type and 0 for the remaining cells of each layer.

***Slope:***

Apart from the abandoned wells, the contaminants can also move into the groundwater system through macropores - root systems, animal burrows, and other systems of openings and cracks that supply pathways for contaminants (Talabi and Kayode 2019). A higher land surface slope allows the surface pollutants to flow rapidly, whereas a lower slope stores these pollutants for a long period which help them travel into these micropores and abandoned wells introducing them into the groundwater systems which accelerates the pollution of the aquifers (Yang and Wang 2010). Low slope increases the risk of contamination whereas high slope decelerates the risk of contaminants entering the aquifer. According to the slope calculated from the digital elevation model, the majority of the area in the GCA region has lower slope with being least at the coastal region (Figure 14).

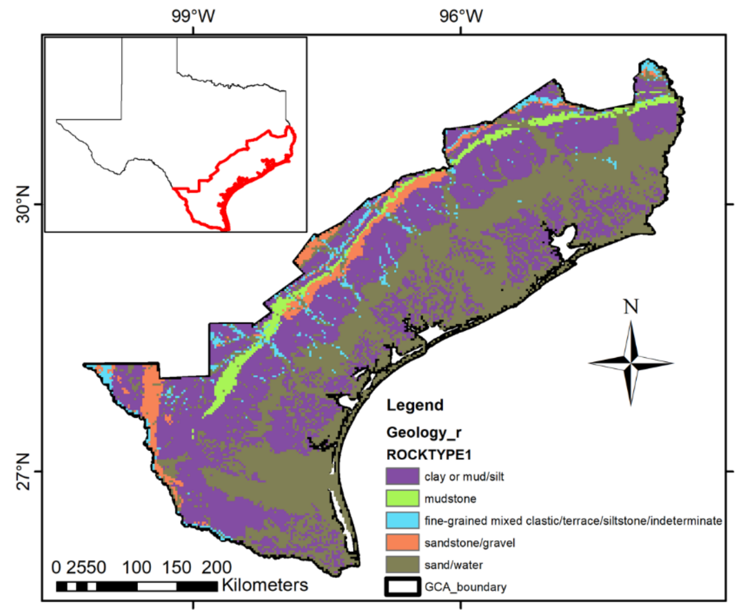


Figure 13 Geology over the GCA system.

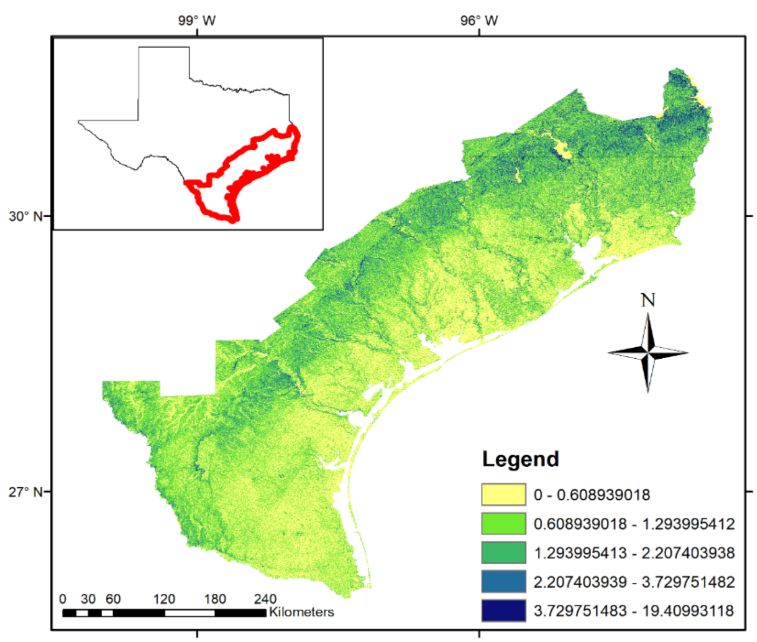


Figure 14 Slope over the GCA system.

#### b. Generalized Linear Regression Model:

Generalized Linear Regression (GLR) is a form of linear least square approach used in statistics to estimate the unknown parameters in a linear regression model. The principle of least square is used by GLR to choose the parameters of a linear function of a set of explanatory variables: minimizing the sum of squares of differences between the observed dependent variable in a dataset and those predicted by the independent variable's linear function (Aspinall 2004). The equation below explains the relationship of the input and output variables of the regression analysis. In this equation, Y is the dependent variable (target), $\beta_o$, $\beta_1$, $\beta_{2,\ldots}$ ,$\beta_{10}$ are the coefficients, $X_1$, $X_{2,\ldots,}$ $X_n$ are the explanatory variables and $\mathcal{E}$ is the random error term or the residuals of the input values (Achmad et al. 2015).

$$\boldsymbol{Y = \beta_o + \beta_1 X_1 + \beta_2 X_2 + \ldots\ldots\ldots + \beta_{10} X_{10} + \mathcal{E}}$$

In this exercise, locations of known contamination sites were used as out target variable. A total of 10 input layers (Abandoned wells, precipitation, geology, slope, wastewater outfalls, petroleum storage tanks, superfund sites, landfill points, streams, and reservoirs) were used as our input variables.

In Texas, there were five abandoned wells which were identified leaking oil, gas and other toxic substances in an amount that poses an immediate risk to environment and public safety by RRC. Four out of these five abandoned wells are located within the GCA region (Figure 15). GLR model used the linear relationship between these four contaminated well locations and the input layers. The generated relationship was then used to predict the vulnerability of entire GCA region.

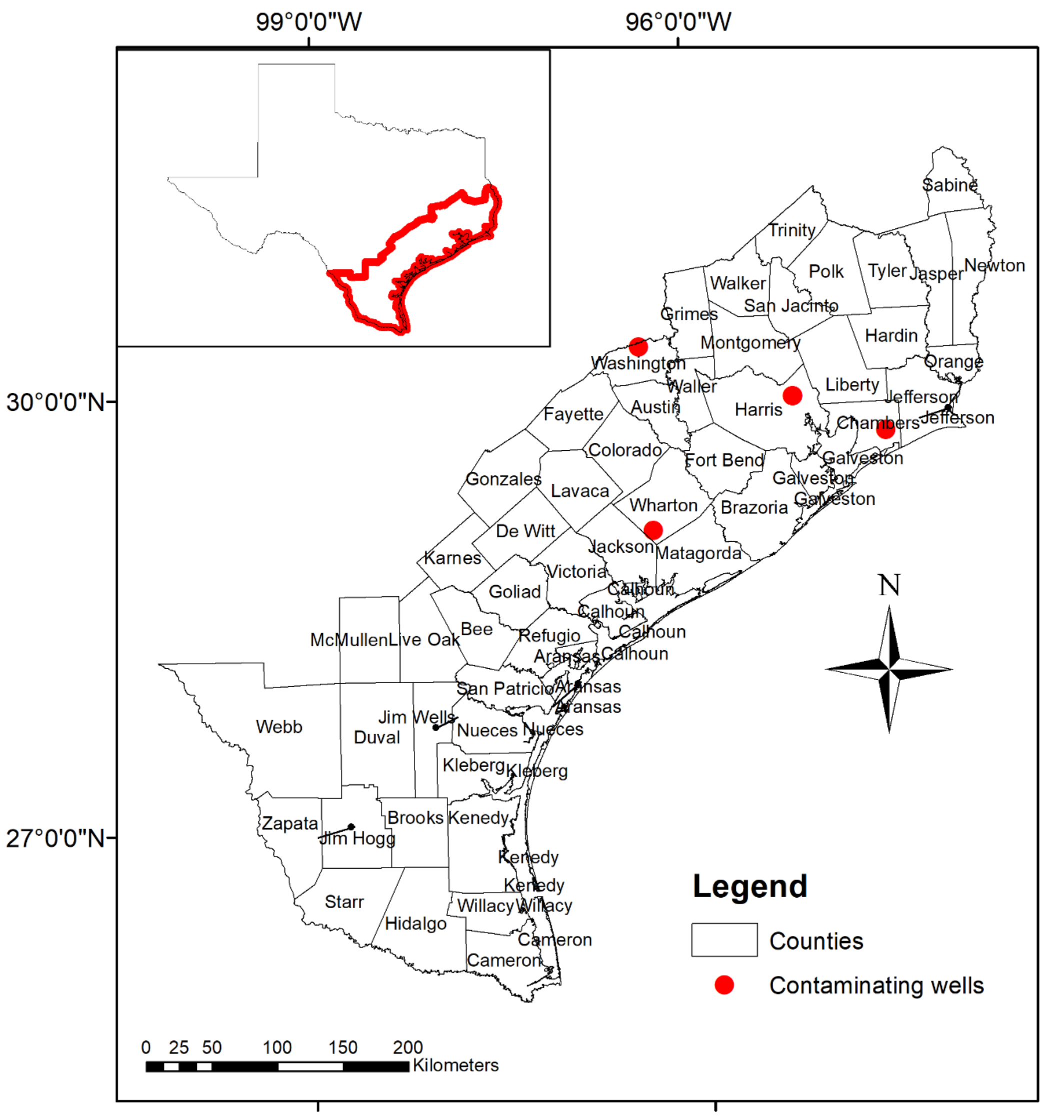


Figure 15 Locations of contaminating abandoned wells over the GCA.

## 2. Geophysical Signature of Abandoned Wells

Two geophysical techniques, magnetic and electromagnetic, were used to characterize the signature of abandoned wells in the field. The main purpose behind this exercise is to use these geophysical responses to locate, and eventually plug, buried abandoned wells in the GCA.

Magnetic methods measure variations in the Earth's magnetic field. This survey provides valuable information about the composition and structure of the earth's crust by reflecting the variations in the magnetic properties of the underlying objects and rocks (Chandra 2015). The unit of the measurement of magnetic field strength is nanotesla (nT). Magnetic data collection can be done by using relative or absolute magnetometers. Total value of earth's magnetic field at a fixed point is measured by an absolute magnetometer and the change in the magnetic field at a point relative to the base station is measured by a relative magnetometer (Roth et al. 1998).

The Geometrics G-858 Magnetometer system was used to acquire magnetic data. A base station was set up at the GTS at a minimum of 100 m away from large metallic objects or traveled roads and at least 500 m away from power lines. Base station readings were used to correct for the diurnal variations in the Earth's magnetic field. Two base station readings were collected, before and after the actual field data acquisition. Acquisition time was recorded for each base station reading.

Magnetic data were collected on a grid consisting of 19 east-west and 5 north-south profiles (Figure 18). Profile separation was set to 2.5m. Magnetic data were collected automatically at a rate of 5 readings per second. We reported data for top sensor, bottom sensor, as well as the vertical gradient between them. GPS data were recorded simultaneously with the magnetic data.

The field magnetic data were downloaded using Magmap software. The same software was used to conduct the diurnal correction of the collected magnetic data. The field data were then extracted in a format compatible with the Surfer software. The latter was used to plot the collected magnetic data.

Figure 16  Electromagnetic data collection over the grid set up at the GTS.

Figure 17 Figure 18 Magnetic data collection setup.

By analyzing variations in the electrical conductivity of rocks, the electromagnetic (EM) technique is commonly used to map subsurface structure and composition. EM methods use transmitters to create powerful time-varying primary magnetic fields in conductive rocks, which enable electrical currents to flow. Secondary electromagnetic fields are created by these currents, which are sensed by receiver antennae (Barsukov and Khabensky 2015). To generate EM fields, there are two main approaches: frequency-domain systems send signals at a variety of frequencies and observe variations in the amplitude and phase of the resultant field, while time-domain systems turn off the primary field abruptly and observe the decay of the generated eddy currents. Electromagnetic surveys can be carried out from the air, on the ground, or via boreholes. (Zhdanov et al. 2013).

The Geonics EM-31 system was used to collect electromagnetic data whose effective depth of exploration is about 6 m. A field grid of 19 east-west and 5 north-south profiles was set at 2.5 m separation. Figure 19 shows the locations of the geophysical profiles collected over the well covers at the GTS. The electromagnetic readings were collected along the setup grids by placing the sensor both in vertical and horizontal positions. The collected data includes imaginary component which is apparent conductivity in milli siemens per meter (mS/m) (also called Quadrature or Out-of-phase) and real component a ratio of secondary to primary magnetic field in parts per thousand (ppt) (also called as In-phase). These data were then downloaded using DAT31W software and converted into Microsoft excel files and plotted using the Surfer software. The real component was completely saturated (20.48 ppt) due to the higher conductivity of the GTS. Hence it is not considered for any further analysis.

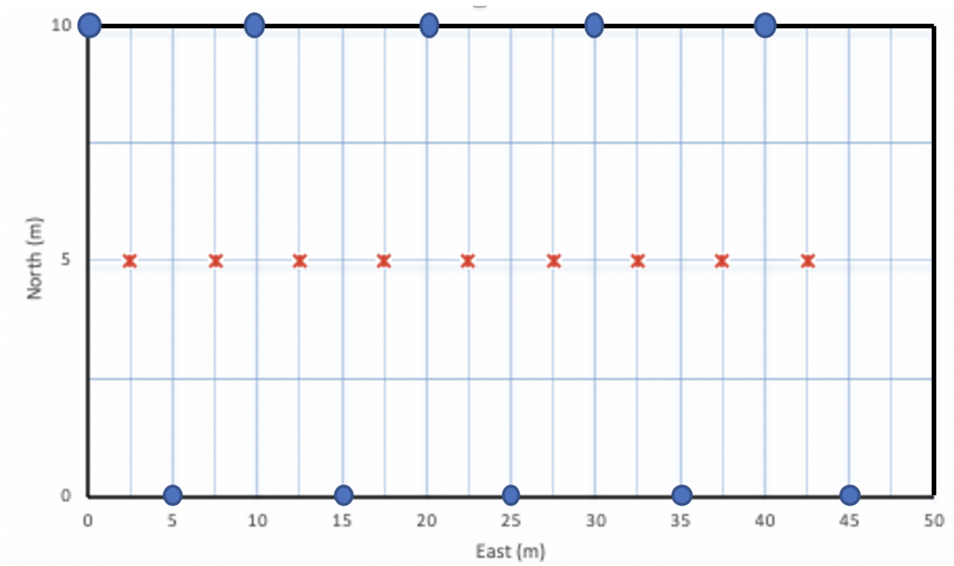


Figure 18 locations of geophysical profiles (blue lines) collected over the targeted well covers at the GTS; objects in red are buried well covers and objects in blue are buried steel drums.

# CHAPTER III

## Results

### 1. Risk Map of GCA due to Abandoned Wells:

By integrating ten input layers for GCA (Table 1), namely precipitation, geology, reservoirs, wastewater outfalls, super fund points, landfill points, steams, slope, petroleum storage tanks, and abandoned wells a vulnerability map was developed (Figure 20). Note the geology were subclassified into 7 different layers (one for each soil type). The risk of contamination was divided into four classes using the minimum (-0.019178), maximum (0.021744), mean (0.002755), and standard deviation (0.004396) of the estimated values of the target variable. Our class limits were mean ± standard deviation. The output cells with values from 0.007115 to 0.021591 were classified as high risk (class 1), 0.002756 to 0.007114 as moderate risk (class 2), -0.001640 to 0.002755 as low risk (class 3), and -0.012600 to -0.001641 as no risk zones (class 4) (Figure 20).

Modelling results indicate that 11.53% of the total area of the GCA region is under high risk of groundwater contamination, whereas 43.79% of the area is at moderate risk, 31.05% of the area is at low risk, and 13.61% of the area is at no risk. The area of the GCA which is at high risk of groundwater pollution due to the abandoned oil and gas wells is mostly centered over the Liberty, Jefferson, Jackson, Live Oak, Zapata, Washington, Calhoun, Chamber, and McMullen counties. These counties are actively producing oil and gas with an average of 1,129,300 to 18,236,889 BBL/year oil and gas extraction (Figure 21). Most of the high-risk area is concentrated around the city of Houston, which is predominantly an industrial area and also known as the world capital of the oil and gas industry. The waste produced from the industries and the ongoing oil and gas production on a large scale could be possible reasons for the high-risk potentiality. The areas which are in the high-risk zone are interpreted to have a high number of abandoned wells, petroleum storage tanks, wastewater outfalls and superfund points, high precipitation, higher slope, high stream density and reservoirs, and mostly contains permeable layers like sand, gravel, and water in the ground which account for the greater chances of groundwater contamination from surface contamination sources.

Areas of the GCA region which are at no risk are mostly concentrated on the southern part. These areas include Duval, Jim Hogg, Webb, Kenedy, Brooks, Lavaca, and Polk counties. These counties have the least oil and gas activities compared to the other counties with 500 to 4,000 BBL/year average annual oil and gas extraction rates which left a very few abandoned wells except for Webb County. Webb County has more than 9,000 BBL/year oil and gas extraction rates but has very few abandoned wells. In the north-western part of the Webb County, there are zero abandoned wells, wastewater outfalls or superfunds and the surface lithology is comprised of mostly clay, which accounted for the least likelihood of ground water contamination due to the abandoned wells.

About 43.79% of the GCA region is at moderate risk of contamination. Although there is no immediate risk associated with these regions, there might be a possibility of future risk of contamination. The abandoned oil and gas wells in these regions need to be properly plugged to avoid any risk of contamination.

Table 1 Summary statistics of each of the GLR input layers. ED is the Euclidean Distance.

| Variable | Coefficient | Unit | Minimum | Maximum | Mean | Standard deviation. |
|---|---|---|---|---|---|---|
| Petroleum Storage Tanks | 0.030834 | ED (°) | 0 | 0.806783 | 0.094009 | 0.084001 |
| Landfill Sites | -0.007656 | ED (°) | 0 | 1.27124 | 0.3603 | 0.219809 |
| Superfund Sites | -0.006524 | ED (°) | 0 | 2.16211 | 0.517125 | 0.38102 |
| Wastewater Outfalls | 0.000197 | ED (°) | 0 | 0.550976 | 0.111725 | 0.099832 |
| Streams | -0.011067 | ED (°) | 0 | 0.4093 | 0.039756 | 0.046824 |
| Reservoirs | -0.007106 | ED (°) | 0 | 1.10474 | 0.31053 | 0.193776 |
| Abandoned Wells | -0.021499 | ED (°) | 0 | 0.816642 | 0.104957 | 0.08671 |
| Slope | 0.000000 | ° | 0 | 9.9264 | 27.013432 | 528.189 |
| Precipitation | 0.000002 | mm | 0 | 1549.4 | 922.0962 | 2915.4882 |
| Sand | -0.013846 | N/A | N/A | N/A | N/A | N/A |
| Terrace | -0.013721 | N/A | N/A | N/A | N/A | N/A |
| Mudstone | -0.008848 | N/A | N/A | N/A | N/A | N/A |
| Water | -0.012952 | N/A | N/A | N/A | N/A | N/A |
| Gravel | -0.006448 | N/A | N/A | N/A | N/A | N/A |
| Silt | -0.014786 | N/A | N/A | N/A | N/A | N/A |
| Clay or Mud | -0.013006 | N/A | N/A | N/A | N/A | N/A |

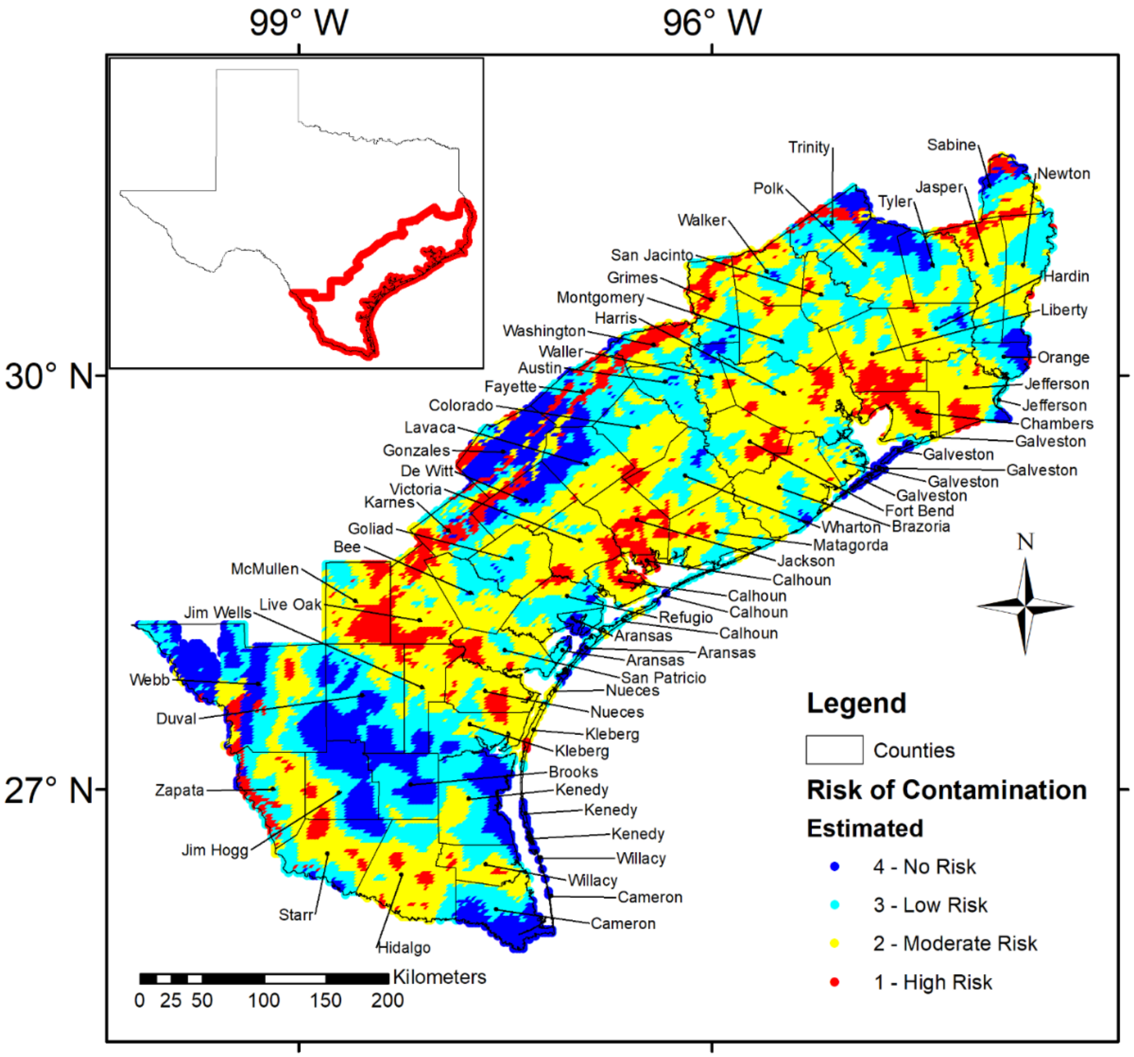


Figure 19 Risk map due to abandoned wells within the GCA. The areas in red color (class # 1) represents the regions which are at high risk, yellow color (class # 2) represents the areas which are at moderate risk, cyan color (class # 3) represents the areas at low risk, and navy blue (class #4) represents the areas at no risk.

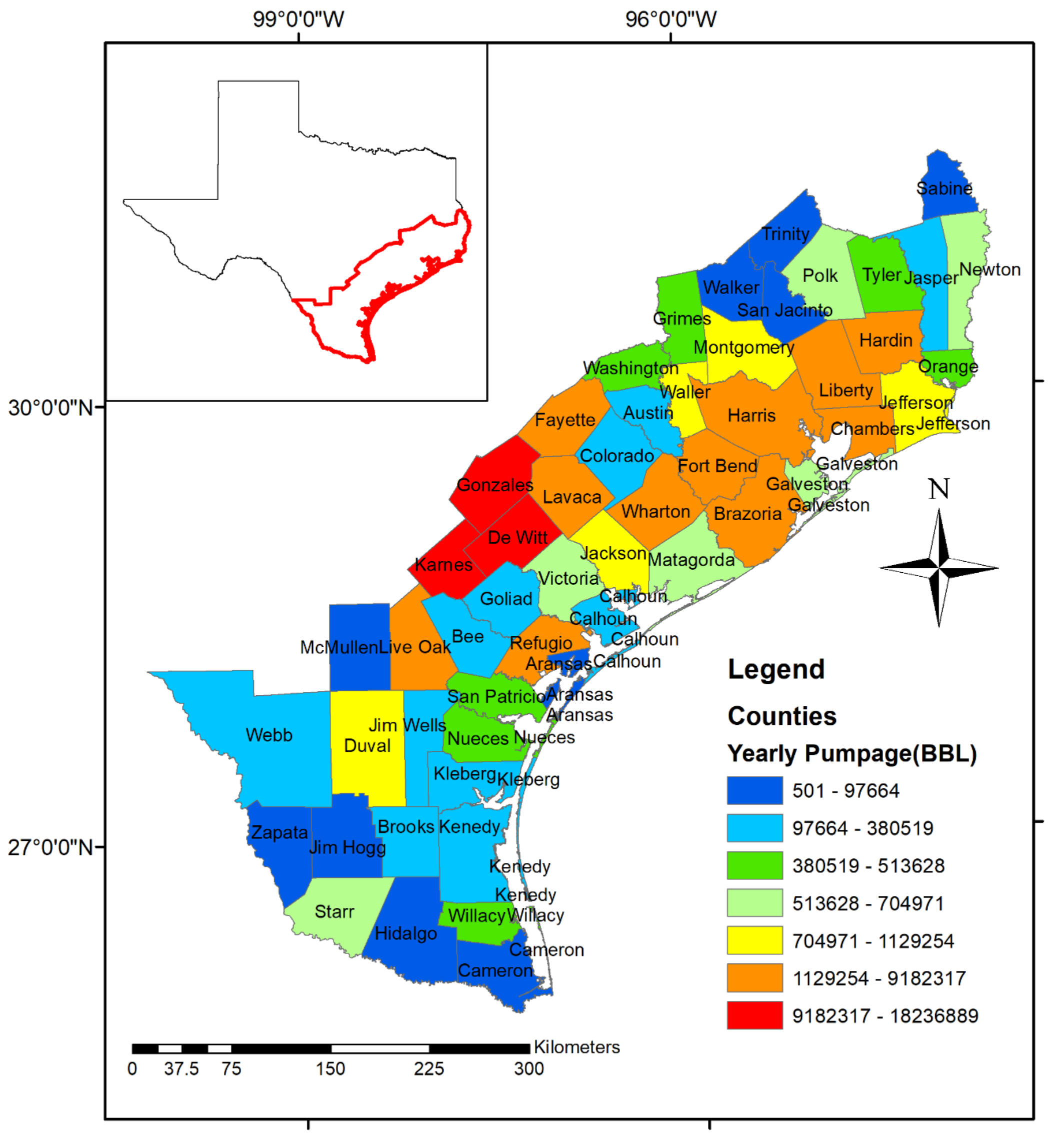


Figure 20 Map depicting the average annual oil and gas extraction rates in the GCA counties during the period from 1993 to 2020. Raw data extracted from Texas Railroad Commission (https://www.rrc.state.tx.us/).

## 2. Geophysical Signature of Abandoned Wells:

It is important to identify a buried well to properly plug it and eliminate the risk of further contamination. To do so, describing the magnetic and electromagnetic anomalies of the buried wells is very important to interpret the magnetic and electromagnetic maps collected over them. The anomalies can be distinguished as fields generated by heterogeneous iron/steel bodies which in this case are the buried drums and well covers.

Magnetic anomalies show a range for the readings of the top and bottom sensors over the buried well covers and the streel drums between 45,700 nT and 44,900 nT. The vertical gradient values ranged from -1,800 to +1,600 nT/m. The range of readings for the bottom sensor is larger compared to the range of readings for the top sensor as the bottom sensor is closer to the ground and thus, closer to the objects.

Visual inspection of Figure 22 indicates that drums 1-10 have doublet circular anomalies with positive and negative polarities above and below 45,300 nT (the average total magnetic field strength of the study area), except for drums 5 and 7. These anomaly shapes are similar for both bottom and top sensors. We were unable to describe the anomaly of the well covers as their signal was interfered by the strong signal from the drums that are much larger in size compared to the well covers. The magnetic field strength depends upon the depth of the object and the orientation (latitude) of the objects as it is a vector quantity. The objects show a higher magnetic field strength when the induced field (object) is parallel earth's field and a lower field strength when the induced magnetic field is perpendicular to the earth's magnetic field (John M. Reynolds 2011). In the magnetic data collected at GTS, the objects buried in NS orientation had higher magnetic signal.

After qualitatively inspecting the magnetic anomalies, we added the layer of buried well covers and the steel drums to validate the results.

To examine the amplitude and the extent of the magnetic anomalies observed over the well covers and the steel drums, the top sensor readings, bottom sensor readings, and the vertical gradient readings were plotted against the longitudes for each profile. The locations of well covers and steel drums were also shown on these profiles (Figure 23). Readings spiked for drums 1, 2, 4, & 5, except drum 3. Drum 2 had the highest reading of 45,750 nT for the top sensor, 47,500 nT for the bottom sensor, and 1,800 nT/m for the vertical gradient, whereas drum 3 had the lowest reading of 44,850 nT for the top sensor, 43,000 nT for the bottom sensor, and 2,000 nT/m for the vertical gradient. The magnetic signatures of the steel drums varied with their orientation, size, and the depth at which they were buried. Table 2 describes the weight, length, depth to top, position, and the orientation of each of the well covers and drums. Magnetic anomalies over drums 1-5 were different due to the difference in their depth of burial and orientation. Drums with north-south orientation produced a stronger signal (average: 45,550 nT) than the drums with east-west orientation (average: 45,350 nT). Though drums 1,4, and 5 are oriented in same direction, drum number 5 had the least signal (average:  45,350 nT) as it is buried at 2 m depth, which is deeper than the other drums.

The readings for top sensor, bottom sensor, and vertical gradient spiked for some well covers but the variations in the readings are not significant due to interference of the signals from the steel drums as discussed earlier. The top sensor reading for well cover 4 was the highest (45,510 nT) and low for the well cover 2 (45,370 nT), the bottom sensor reading is also highest for well cover 4 (45,550 nT) and low for well cover 9 (45,300 nT) (Figure 24).

Table 2 Description of the well covers and the drums.

| No. | Profile | North(m) | Object | Depth to top (m) | Orientation |
|---|---|---|---|---|---|
| 1 | 1 | 5 | 55 gal empty steel drum | 0.5 | Long Axis EW |
| 2 | 1 | 15 | 55 gal empty steel drum | 0.5 | Long Axis NS |
| 3 | 1 | 25 | 55 gal empty steel drum | 0.5 | Long Axis Vert |
| 4 | 1 | 35 | 55 gal empty steel drum | 1.0 | Long Axis EW |
| 5 | 1 | 45 | 55 gal empty steel drum | 2.0 | Long Axis EW |
| 6 | 2 | 2.5 | 6" OD cast iron, 7.5" iron skirt | 2.5 | 8 lb |
| 7 | 2 | 7.5 | 6" cast iron, 7.5" sheet iron skirt | 1.5 | 8 lb |
| 8 | 2 | 12.5 | 6" cast iron, 7.5" iron skirt | 0.5 | 8 lb |
| 9 | 2 | 17.5 | 10" OD cast iron, 12" Fe skirt | 2.5 | 16 lb |
| 10 | 2 | 22.5 | 10" cast iron, 12" sheet Fe skirt | 1.5 | 16 lb |
| 11 | 2 | 27.5 | 10" cast iron, 12" iron skirt | 0.5 | 16 lb |
| 12 | 2 | 32.5 | 8" OD cast Al, cast Al skirt | 2.5 | 5 lb |
| 13 | 2 | 37.5 | 8” cast Al, 7.5" cast Al skirt | 1.5 | 5 lb |
| 14 | 2 | 42.5 | 8” cast Al, 7.5" cast Al skirt | 0.5 | 5 lb |
| 15 | 3 | 0 | 55 gal steel x 2, empty; painted | 2.0 | Both Axes EW, parallel |
| 16 | 3 | 10 | 55 gal steel x 2, empty; painted | 2.8 | Upright, adjacent EW |
| 17 | 3 | 20 | 55 gal steel x 2, empty; painted | 3.0 | Axes NS, par., 1m sep. |
| 18 | 3 | 30 | 55 gal x 3, crushed | 3.0 | Random |
| 19 | 3 | 40 | 55 gal x 3, empty; painted | 3.0 | NS, triang contact |

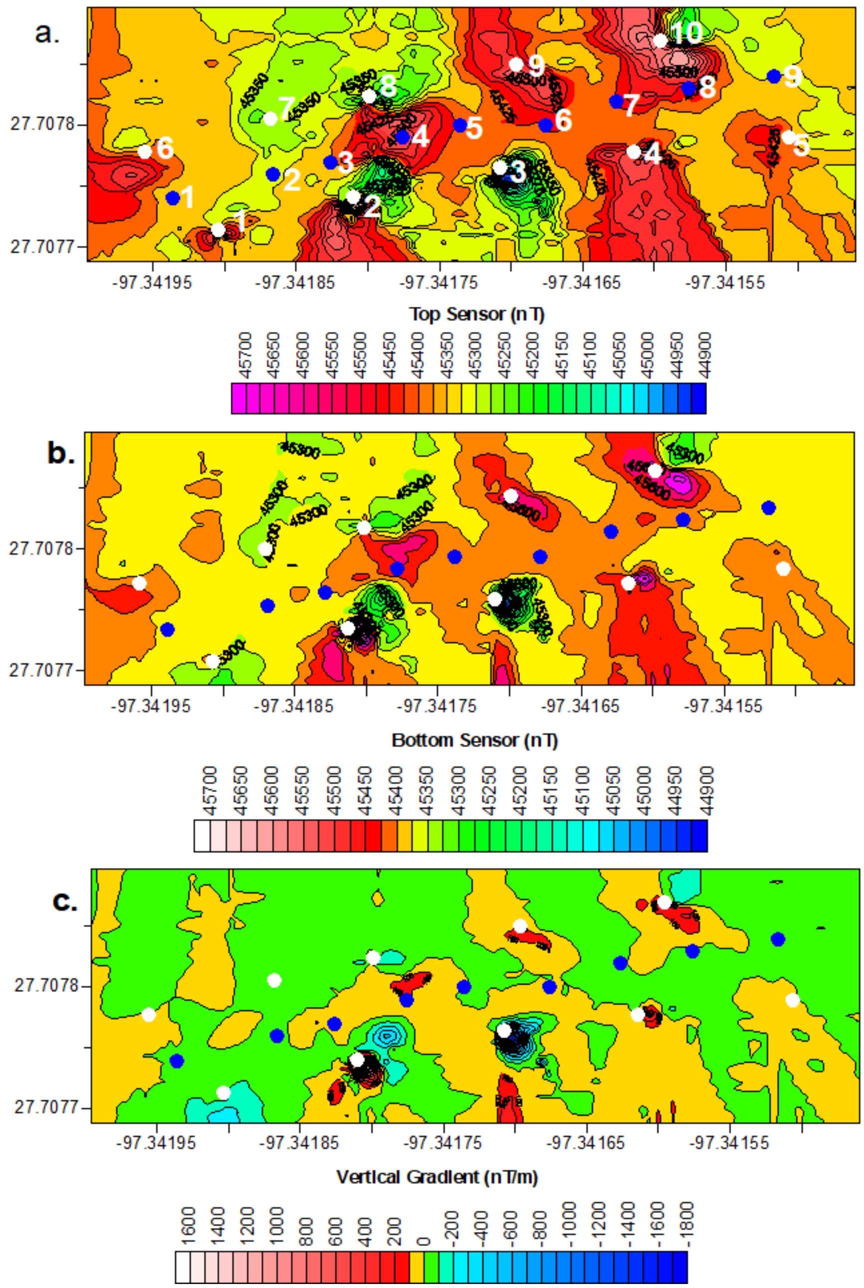


Figure 21 Total magnetic field map from the (a) top sensor, (b) bottom sensor, and (c) vertical gradient. The blue dots in the map represent the buried well covers and the white dots represent the buried steel drums in the GTS.

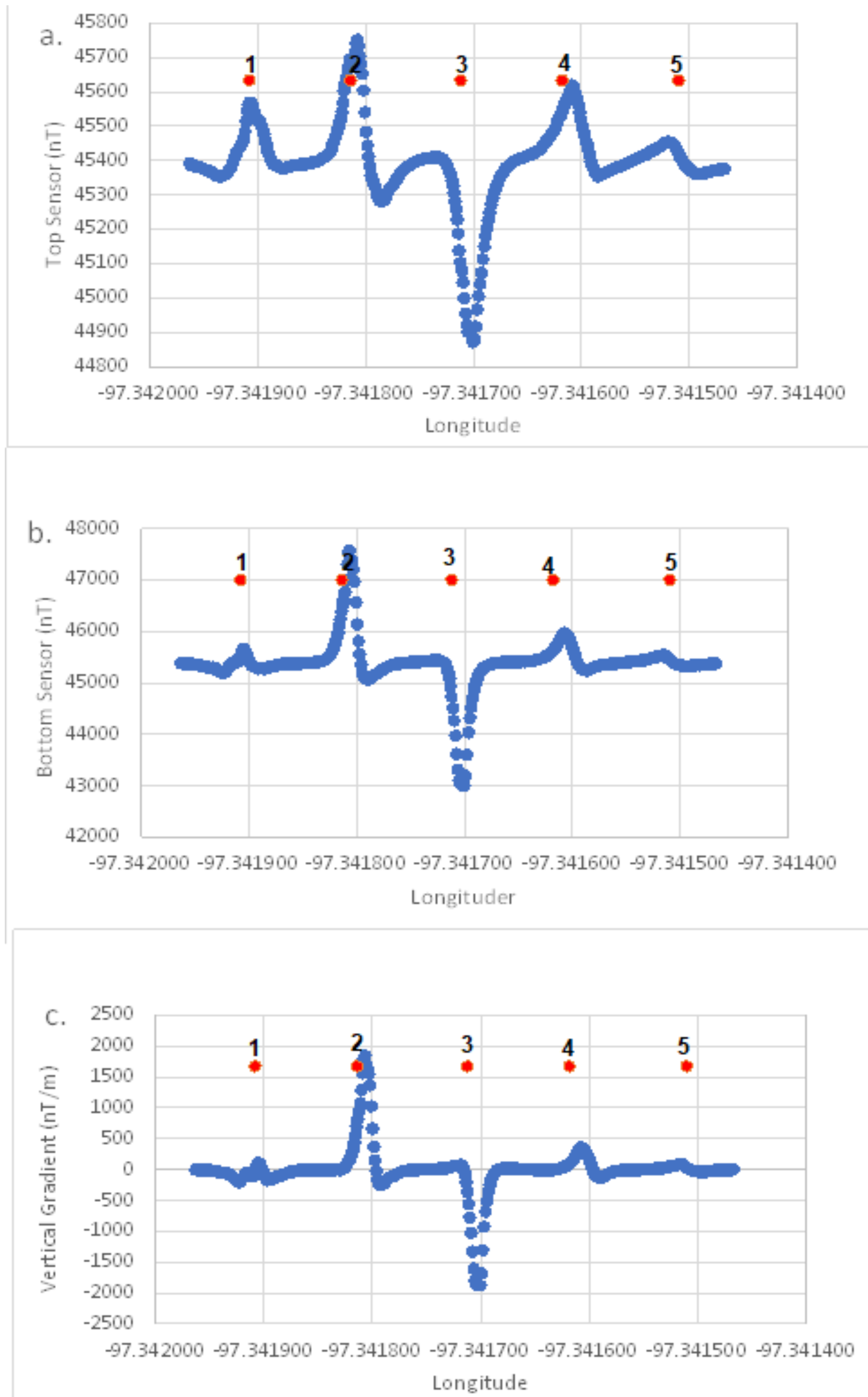


Figure 22 Magnetic profile generated from (a) top sensor, (b) bottom sensor, and (c) vertical gradient over the steel drums buried along and/or close to profile 1.

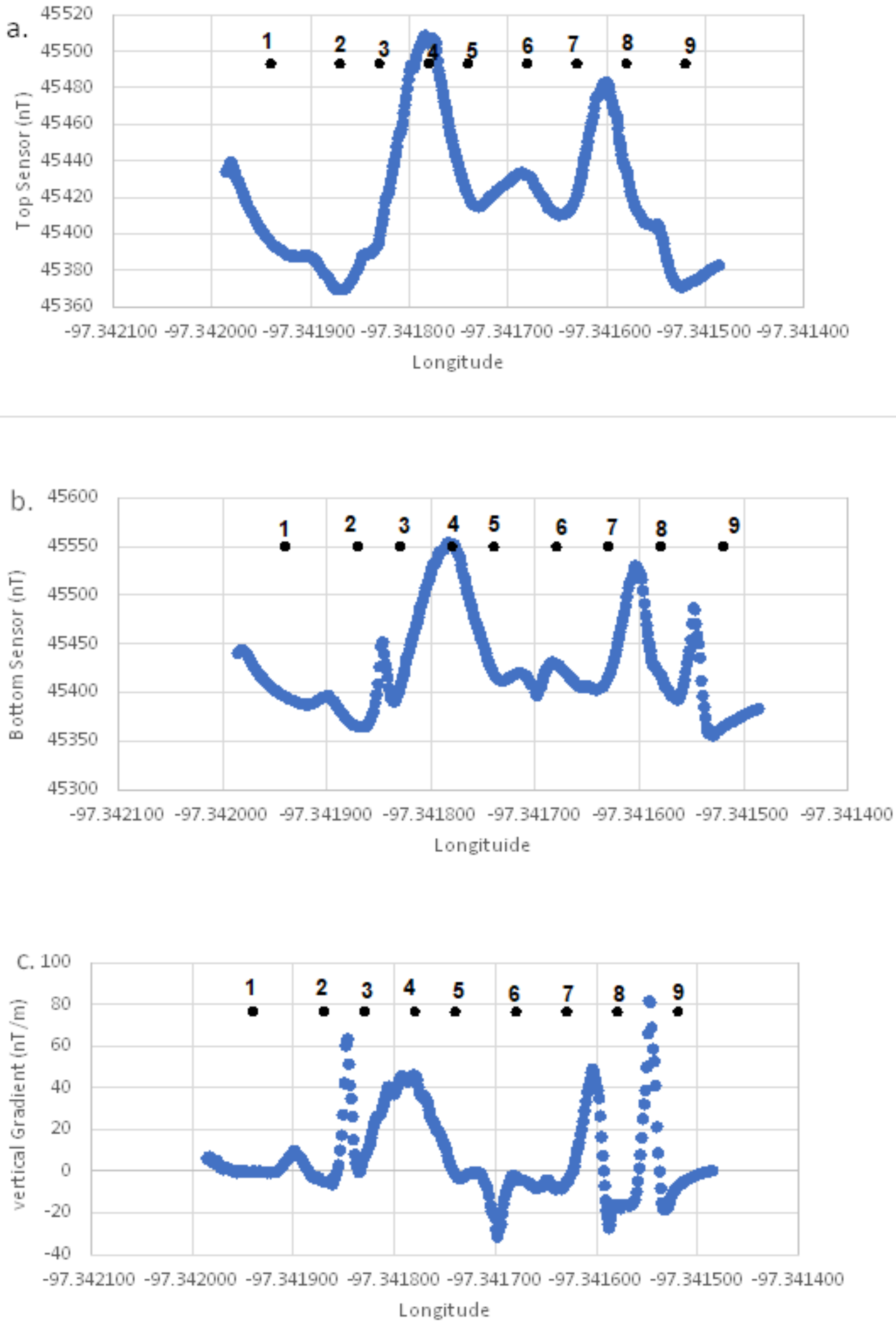


Figure 23 Magnetic profile generated from (a) top sensor, (b) bottom sensor, and (c) vertical gradient over the well covers buried along and /or close to profile 2.

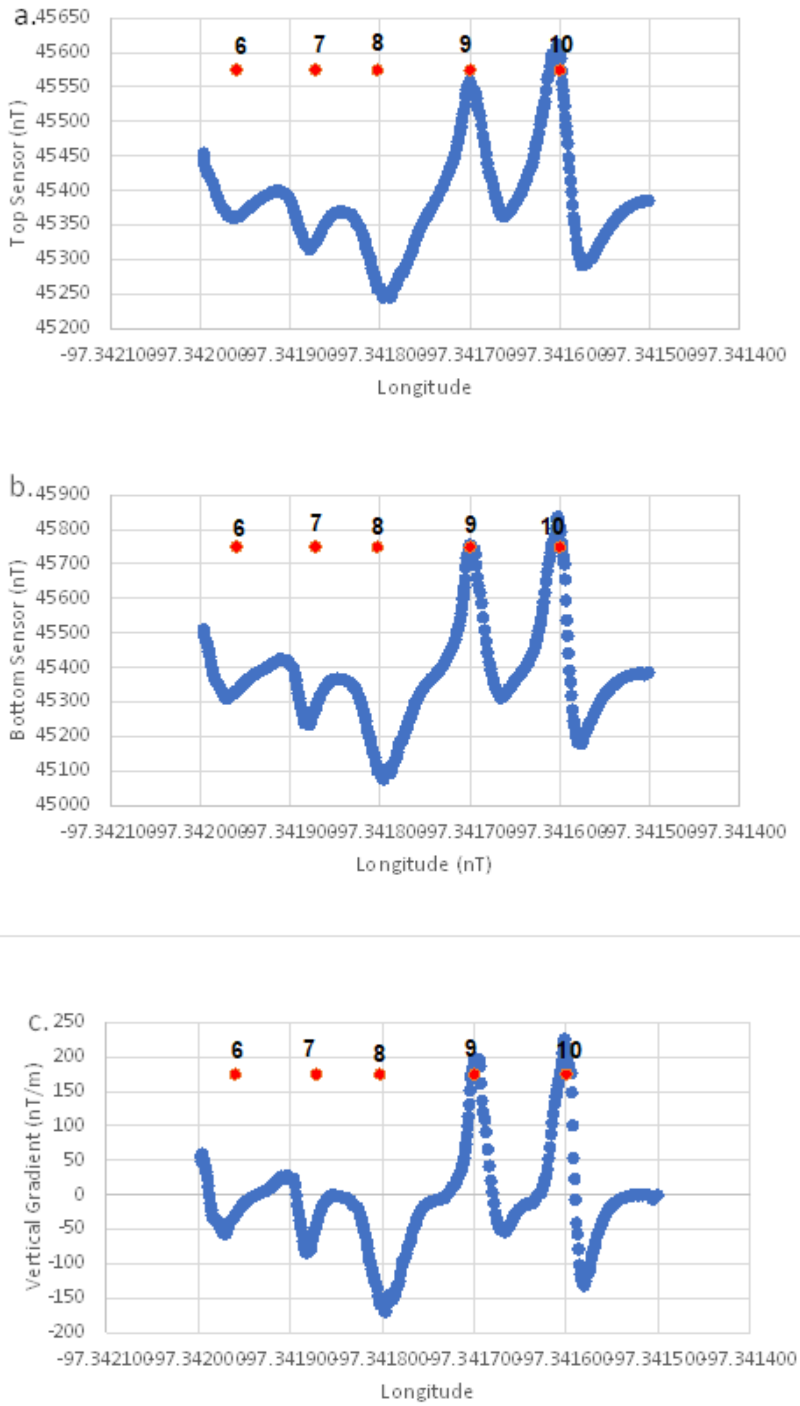


Figure 24 Magnetic profile generated from (a) top sensor, (b) bottom sensor, and (c) vertical gradient over the steel drums buried along and/or close to profile 3.

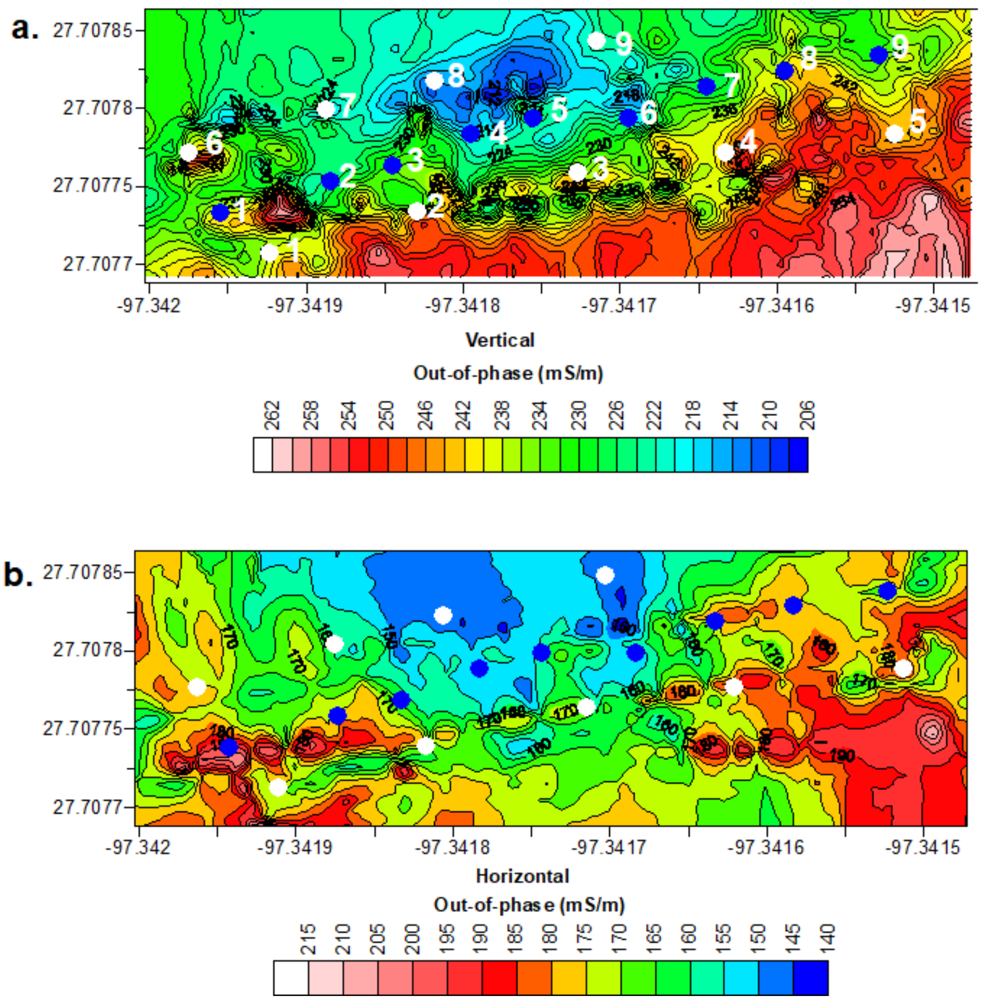


Figure 25 Total electromagnetic map for thee (a) horizontal out-of-phase readings and (b) vertical out-of-phase readings. The blue dots in the map represent the buried well covers and the white dots represent the buried steel drums in the GTS.

Drums buried along profile 3 are marked on the graphs plotted with top, bottom, and vertical gradient readings along profile 3 against longitude in figure 25. Drum 5 had the highest while drum 3 has the lowest readings for all three data. The highest readings were 45,620 nT, 45,850 nT, and 220 nT/m and the lowest readings were 45,220 nT, 45,050 nT, and -170 nT/m for top sensor, bottom sensor, and vertical gradient respectively. Drums 6 through 10 are buried at different orientation, some are even oriented randomly. Drums 6, 9, and 10 showed stronger signals (average: 45,650 nT) and this might be because drum number 6 is buried at a shallow depth of 2 m while the other drums are buried at 2.8 and 3.0 meters depth. These conclusions are based upon the signal received by the top and bottom sensors.

The terrain conductivity of the imaginary (also called quadrature) out-of-phase component (mS/m) measured in vertical configuration and horizontal configuration was plotted using surfer software (figure 26) Electromagnetic anomaly readings, used to identify the signature of the buried well covers, of the vertical out-of-phase ranged from 206 to 266 mS/m. The horizontal out-of-phase readings were between 140 and 215 mS/m. Examination of these maps indicated that there is a strong interference of the signal from the subsurface lithologic layers such as layers of clay (Thomas 2010).

We also graphed the readings of the vertical and the horizontal out-of-phase components against the longitudes for each profile and displayed the buried well covers and the steel drums to describe the interference of the signal from steel drums (Figures 27 - 29). Conductivity readings spiked for some of the drums and well covers based upon their depth of burial, orientation, and the size as discussed in the magnetic section. For the vertical component of profile 1, drum 4 had the highest values (255 mS/m) and drum 2 had the lowest value (223 mS/m). Drums 4 and 5 had the highest values (197 mS/m) and drum 1 had the least value (163 mS/m) for the horizontal component. Drums 1, 4, and 5 are buried in EW direction whereas drums 2 and 3 in NS and vertical positions. In profile 2, values spiked a little near the well covers but there is a significant difference between the vertical and horizontal readings. Well covers 8 and 9 had the highest value (250 mS/m) for vertical component and well cover 1 had the highest value (205 mS/m) for the horizontal component. For profile 3, there was a spike near all the drums, drums 6 and 10 transmitted a higher signal for both vertical (238 mS/m) and horizontal (187mS/m) components. Drum 6 also in the EW orientation. and drum 10 is oriented NS.

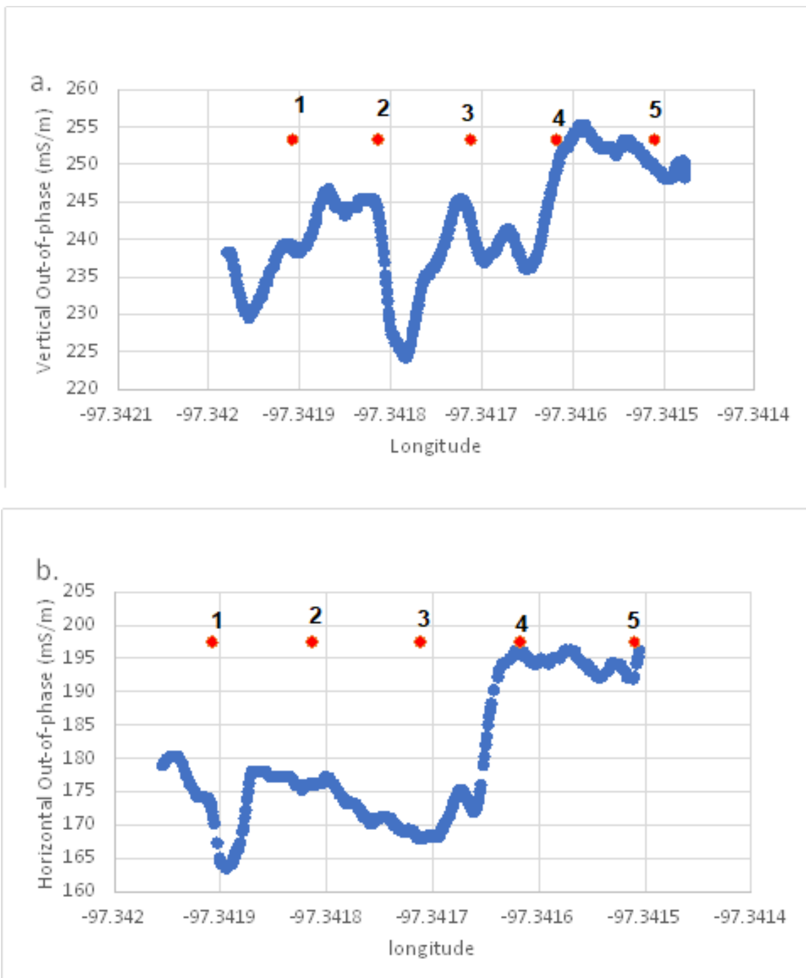


Figure 26 Electromagnetic profile generated from (a) vertical out-of-phase, (b) horizontal out-of-phase over the steel drums buried along and/or close to profile 1.

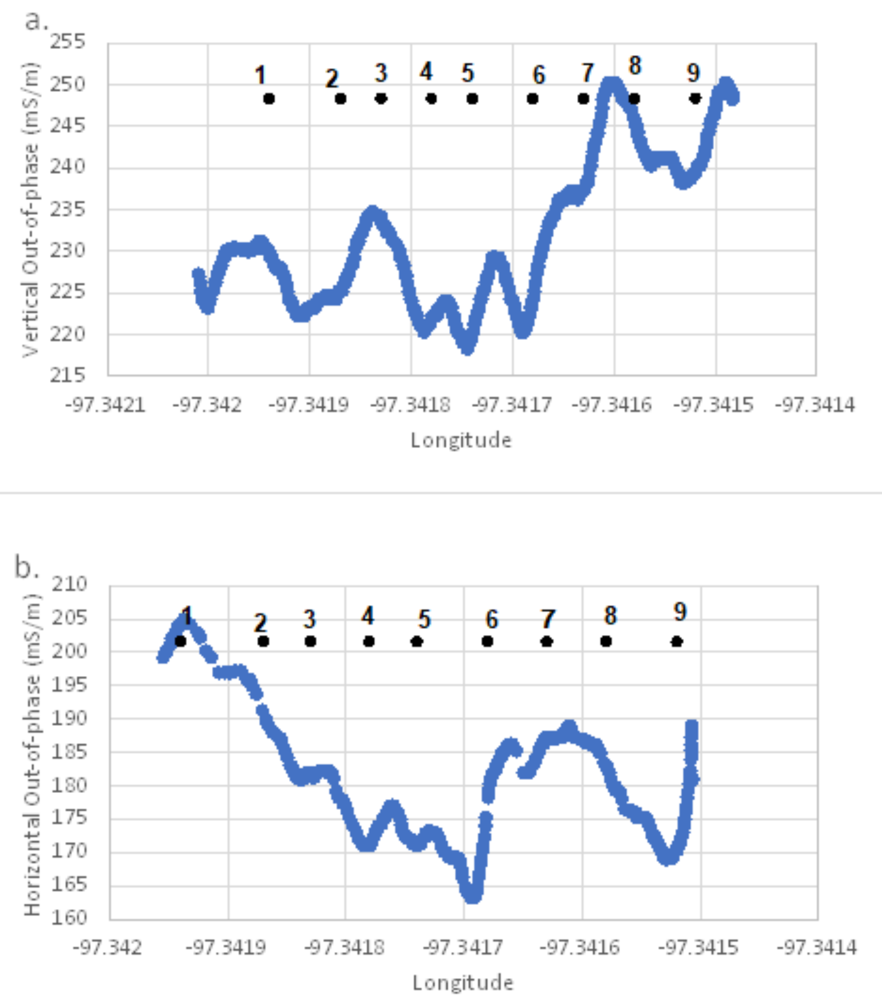


Figure 27 Electromagnetic profile generated from (a) vertical out-of-phase, (b) horizontal out-of-phase over the well covers buried along and/or close to profile 2.

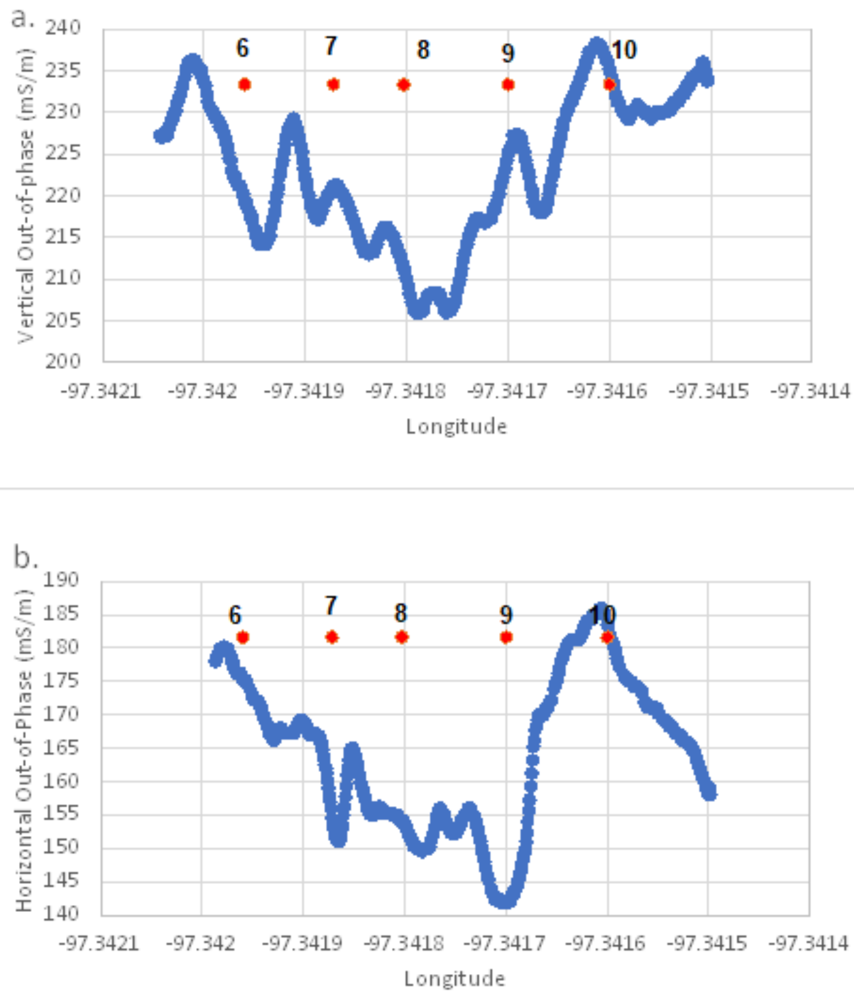


Figure 28 Electromagnetic profile generated from (a) vertical out-of-phase, (b) horizontal out-of-phase over the steel drums buried along and/or close to profile 3.

# CHAPTER IV

## Discussion and Conclusion

As protecting the environment is of utmost importance, this research has many societal benefits. The groundwater supplies drinking water for 51% of the total U.S. population and 99% of the rural population, and helps grow their food, with about 64% of groundwater being used for irrigation to grow crops (More 2015). Groundwater is an important component in many industrial processes and also a source of recharge for lakes, rivers, wetlands, and coastal waters. Contamination of groundwater has various adverse effects such as a lack of water supply, deteriorated surface water systems given their connections, high cleanup expenses, poor drinking water quality, and potential health issues to humans, flora, and fauna. As groundwater is a main source of drinking water around the globe, contaminated groundwater can cause serious health issues like hepatitis, cholera, and methemoglobinemia (Kresic 2020) and the GCA is a major groundwater source for Texas with an estimated total groundwater storage of 6300 $km^3$ as of 2016. The estimated recoverable groundwater storage is between 25 and 75%, which is about 1480 $km^3$ to 4687 $km^3$ (Bruun et al. 2016). With this research, we were able to identify the areas which are prone to the risk of contamination due to abandoned wells within the GCA region. Thus, mitigation activities like plugging can be done to protect the groundwater and surface environment within these areas. Specially in Cameron, Galveston, Harris, and Jefferson counties where 19%, 2%, 33%, and 21% of total municipal use is supplied by groundwater (Fab Flour 2015).

Although our research focused on surface contamination sources, it could also be used to account for subsurface contamination. The surface contaminants are carried to the underground through open abandoned wells which pollute the aquifers (Zaporozec 1981). The water reaches the aquifer via runoff from precipitation and overflow of rivers or reservoirs carrying the contaminants directly to the aquifer. These contaminants can also be transferred into the aquifer from abandoned wells or from one aquifer unit to another aquifer unit through lateral flow or subsurface faults, high hydraulic conductivity (LeGrand 1964). High water flow and moisture retained in the ground can cause corrosion of the well casings which release contaminants into the aquifer through horizontal percolation (Abdalla and Shamrukh 2016). All the input layers were discussed as how they can prove to be productive in increasing the accuracy of the modelling.

The RRC and Texas TCEQ have been plugging the abandoned wells in Texas for years. This research classified the risk zones into high, moderate, low-risk, and no-risk zones, which can be used to prioritize mitigation activities (e.g., plug the wells in the high-risk zones first) to avoid further damage to the groundwater resources and the entire environment. The high-risk zones need immediate attention compared to the low-risk zones.

The TWBD provides water quality data based on tests performed on the surface- and groundwater for chemical compositions. This research can be used as one of the attributes to guide TWDB's activities. Our research results could help TWDB locate the possible causes for the degraded groundwater quality in high-risk zones and perform additional lab investigations to observe the quality of groundwater in that particular region.

Stakeholders and decision-makers can use the results of our geophysical investigation to efficiently locate abandoned wells using non-invasive geophysical techniques such as magnetic and electromagnetic methods. This will enable development and implementation management protocols leading to successful mitigation of risks of abandoned wells while increasing protection of the local environment.

This study has some limitations. In mapping the risk of groundwater contamination in the GCA, we have used the GLR model which is a linear model. Comparing the resulted risk map to other maps generated using different model types such as non-linear models (e.g., Point Processing Modelling, Artificial Neural Network, and Fuzzy logic) would help us better understand the results. The GLR method adapted can be further enhanced by adapting advanced techniques such as machine learning and artificial intelligence.

The model calibration based on four events which are all located in northern and central parts of the GCA can be made more efficient if we could acquire the data of more cases of contamination of groundwater due to abandoned wells in different counties or locations. Though most of the sources of contamination are on the surface, subsurface input layers such as subsurface faults, aquifer lithology, depth of wells, aquifer depth, and hydraulic conductivity can play a significant role in accelerating or decelerating the subsurface contamination (Gangopadhyay et al. 1999). Adding these input layers to our model, if records or data were available, would provide more accurate results.

In addition, the spatial resolution of our model inputs is different for each input, acquiring data with identical spatial resolution for input layers could improve the efficiency of the model (Hardy et al. 1999). For additional calibration, water quality data from TWDB can be acquired to compare the water quality against the risk zones of our results.

Magnetic and electromagnetic signatures of the abandoned wells are not well defined in this study. One of the possible reasons for this is that the well covers are buried in between steel drums which are larger in size and producing larger signals comparing to the well covers. In contrast, in a real-world situation, the well cover will be attached to an entire well which would yield a stronger signal for both magnetic and electromagnetic methods and will produce rather sharp anomalies and make it easy to spot the well. More accurate geophysical results might also be achieved by decreasing the profile interval in the data collection, for instance the data collected with a 0.5 m profile interval would give more opportunities for us to differentiate between the signal from well covers and the steel drums.

Our electromagnetic anomalies could not help us differentiate the signal of the buried objects as the signal from background lithology was dominating (clay layer with higher electric conductivity). This could have been avoided if we had data collected by surveying at the test site before installation of the subsurface objects (well covers, drums). Subtracting the data collected before installation of the objects from the data collected after installing the objects will eliminate the site conductivity and leave the conductivity of the buried objects and would give us the signal from the buried objects. Thus, the anomalies from the objects would be possible to analyze and further examine.

Our geophysical data were collected by ground survey for both magnetic and electromagnetic techniques and airborne surveys or marine surveys could be done to collect the data for a well buried under water or over a large area (e.g., Texas, United States) (Zou et al. 2013). Apart from the magnetic and electromagnetic methods, methods such as electrical resistivity, and ground penetrating radar can also be used to locate the abandoned wells at the surface or buried underground (Hoover et al. 1995).Advanced data processing techniques like 3-D analytic signal of the magnetic data could be adapted for additional research to help show the location of the buried well and its depth underground (Roest et al. 1992).

## REFERENCES


Abdalla F, Shamrukh M (2016) Quantification of River Nile/Quaternary aquifer exchanges via riverbank filtration by hydrochemical and biological indicators, Assiut, Egypt. J Earth Syst Sci 125:1697–1711. https://doi.org/10.1007/s12040-016-0755-1

Achmad A, Hasyim S, Dahlan B, Aulia DN (2015) Modeling of urban growth in tsunami-prone city using logistic regression: Analysis of Banda Aceh, Indonesia. Appl Geogr 62:237–246. https://doi.org/10.1016/j.apgeog.2015.05.001

Acreman M (2000) Managed Flood Releases from Reservoirs: Issues and Guidance Prepared for Thematic Review II.1: Dams, ecosystem functions and environmental restoration Go Back

Ahmed M, Turner R, Haley M, et al (2021) Constructing a geophysical test site for a coastal community's research and education activities. Lead Edge 40:208–215. https://doi.org/10.1190/tle40030208.1

Anderson DJ, Rahman PF, Davey EK, et al (2013) Background Paper on Groundwater Resources in Relation to Coal Seam Gas Production

Aspinall R (2004) Modelling land use change with generalized linear models - A multi-model analysis of change between 1860 and 2000 in Gallatin Valley, Montana. J Environ Manage 72:91–103. https://doi.org/10.1016/j.jenvman.2004.02.009

Banga T, Capuano RM, Bissada KK (2011) Petroleum generation in the southeast Texas basin: Implications for hydrocarbon occurrence at the South Liberty salt dome. Am Assoc Pet Geol Bull 95:1257–1291. https://doi.org/10.1306/11051007036

Barilari A, Quiroz Londoño M, Paris M del C, et al (2020) Groundwater contamination from point sources. A hazard index to protect water supply wells in intermediate cities. Groundw

Sustain Dev 10:100363. https://doi.org/10.1016/J.GSD.2020.100363

Barsukov PO, Khabensky EO (2015) Shallow Investigations by TEM-FAST Technique : Methodology and Exam- ples A Review of Airborne Electromagnetic Methods With Focus on Geotechnical and Hydrological Applications From 2007 to 2017

Bruun B, Jackson K, Lake P, Walker J (2016) Texas Aquifers Study: Groundwater Quantity, Quality, Flow, and Contributions to Surface Water. 304

Callahan CA, Menzie CA, Burmaster DE, et al (1991) On-site methods for assessing chemical impact on the soil environment using earthworms: A case study at the baird and McGuire Superfund Site, Holbrook, Massachusetts. Environ Toxicol Chem 10:817–826. https://doi.org/https://doi.org/10.1002/etc.5620100612

Chandra P (2015) The magnetic method. Groundw Geophys Hard Rock 63–85. https://doi.org/10.1201/b19255-6

Davies RJ, Almond S, Ward RS, et al (2014) Oil and gas wells and their integrity: Implications for shale and unconventional resource exploitation. Mar Pet Geol 56:239–254. https://doi.org/10.1016/j.marpetgeo.2014.03.001

Edwards Aquifer Authority (2019) No Title. In: Abandon. Well Initiat.

Fab Flour (2015) Facts About. FabflourCoUk/Fab-Bread/Facts-About-Bread/ 1–2

Galloway D, Jones DR, Ingebritsen SE (2000) Land subsidence in the United States. US Geol Surv Circ 1–175

Gangopadhyay S, Gautam TR, Gupta A Das (1999) Subsurface Characterization Using Artificial Neural Network and GIS. J Comput Civ Eng 13:153–161. https://doi.org/10.1061/(ASCE)0887-3801(1999)13:3(153)

Haley JL, Lang DJ, Herrinton L (1989) EPA's Approach to Evaluating and Cleaning Up Ground Water Contamination at Superfund Sites. Groundw Monit Remediat 9:177–183. https://doi.org/https://doi.org/10.1111/j.1745-6592.1989.tb01027.x

Hardy RJ, Bates PD, Anderson MG (1999) The importance of spatial resolution in hydraulic models for floodplain environments. J Hydrol 216:124–136. https://doi.org/10.1016/S0022-1694(99)00002-5

Harris BL, Hoffman DW, Mazac Jr FJ, Mazac FJ (1996) Reducing the Risk of Ground Water Contamination by Improving Pesticide Storage and Handling

Hillebrand S, Fish US (2018) Abandoned Wells What happens to oil and gas wells when they are no longer productive? 1–2

Hoover DB, Klein DP, Campbell DC (1995) GEOPHYSICAL METHODS IN EXPLORATION AND MINERAL ENVIRONMENTAL INVESTIGATIONS

Hussein S, Abdelkareem M, Hussein R, Askalany M (2019) Using remote sensing data for predicting potential areas to flash flood hazards and water resources. Remote Sens Appl Soc Environ 16:100254. https://doi.org/10.1016/j.rsase.2019.100254

Jerrett M, Burnett RT, Kanaroglou P, et al (2016) A GIS–Environmental Justice Analysis of Particulate Air Pollution in Hamilton, Canada: http://dx.doi.org/101068/a33137 33:955–973. https://doi.org/10.1068/A33137

John M. Reynolds (2011) An Introduction to Applied and Environmental Geophysics 2nd Edition. John Wiley Sons, Ltd 193

Khodadad S, Jang D-H (2015) A comparative study of Analytical Hierarchy Process and Ordinary Least Square methods for landslide susceptibility mapping using GIS technology.

TOJSAT 5:7–16

King G (2012) Representative, Environmentalist, Regulator, Reporter, Investor, University Researcher, Neighbor and Engineer Should Know About Estimating Frac Risk and Improving Frac. SPE Hydraul Fract Technol Conf SPE 152596

King GE, Valencia RL (2014) Environmental Risk and Well Integrity of Plugged and Abandoned Wells

Kresic N (2020) Groundwater Contamination. Hydrogeol Groundw Model 425–468. https://doi.org/10.1201/9781420004991-9

LeGrand HE (1964) System for Evaluation of Contamination Potential of Some Waste Disposal Sites. J Am Water Works Assoc 56:959–974. https://doi.org/10.1002/j.1551-8833.1964.tb01292.x

Mace RE, Davidson SC, Angle ES (2006) Texas Water Development Board Report 365 Aquifers of the Gulf Coast of Texas edited by

Maxwell RM, Kastenberg WE (1999) Stochastic environmental risk analysis: An integrated methodology for predicting cancer risk from contaminated groundwater. Stoch Environ Res Risk Assess 13:27–47. https://doi.org/10.1007/s004770050030

Mollalo A, Mao L, Rashidi P, Glass GE (2019) A gis-based artificial neural network model for spatial distribution of tuberculosis across the continental united states. Int J Environ Res Public Health 16:1–17. https://doi.org/10.3390/ijerph16010157

More R (2015) The Basics What is Groundwater ? How much do we depend on groundwater ? 99

Nellis MD, Harrington JA, Wu J (1998) Remote sensing of temporal and spatial variations in pool size, suspended sediment, turbidity, and Secchi depth in Tuttle Creek Reservoir, Kansas: 1993. Geomorphology 21:281–293. https://doi.org/10.1016/s0169-555x(97)00067-6

Nicot J-P (2008) A survey of oil and gas wells in the Texas Gulf Coast, USA, and implications for geological sequestration of CO2. Environ Geol 2008 577 57:1625–1638. https://doi.org/10.1007/S00254-008-1444-4

Palmer MA, Menninger HL (2013) Invertebrates, Freshwater, Overview. Encycl Biodivers Second Ed 369–378. https://doi.org/10.1016/B978-0-12-384719-5.00077-0

Pátzay G, Kármán FH, Póta G (2003) Preliminary investigations of scaling and corrosion in high enthalpy geothermal wells in Hungary. Geothermics 32:627–638. https://doi.org/10.1016/S0375-6505(03)00068-3

Rana R, Ganguly R, Gupta AK (2018) Indexing method for assessment of pollution potential of leachate from non-engineered landfill sites and its effect on ground water quality. Environ Monit Assess 190:. https://doi.org/10.1007/s10661-017-6417-1

Reedy RC, Scanlon BR, Walden S, Strassberg G (2011) Naturally Occurring Groundwater Contamination in Texas

Reforms R (2011) State Oil and Gas Agency Groundwater Investigations. 165

Roest WR, Verhoef J, Pilkington M (1992) Magnetic interpretation using the 3-D analytic signal. GEOPHYSICS 57:116–125. https://doi.org/10.1190/1.1443174

Roth BJ, Sepulveda NG, Jr. JPW (1998) Using a magnetometer to image a two-dimensional current distribution. J Appl Phys 65:361. https://doi.org/10.1063/1.342549

RRC (2021a) well plugging. https://www.rrc.texas.gov/news/092320-well-plugging/. Accessed

20 Oct 2021

RRC (2021b) The Railroad Commission of Texas. https://www.rrc.state.tx.us/. Accessed 21 Oct 2021

Sierraclub (2004) Leaking Underground Storage Tanks : A Threat to Public Health & Environment Quality

Talabi AO, Kayode TJ (2019) Groundwater Pollution and Remediation. J Water Resour Prot 11:1–19. https://doi.org/10.4236/jwarp.2019.111001

Teng Y, Feng D, Song L, et al (2013) Total petroleum hydrocarbon distribution in soils and groundwater in Songyuan oilfield, Northeast China. Environ Monit Assess 185:9559–9569. https://doi.org/10.1007/s10661-013-3274-4

Thomas AM (2010) Measurement of Electromagnetic Signal Velocities in Saturated Fine-Grained Soils

Vrålstad T, Saasen A, Fjær E, et al (2019) Plug & abandonment of offshore wells: Ensuring long-term well integrity and cost-efficiency. J Pet Sci Eng 173:478–491. https://doi.org/10.1016/j.petrol.2018.10.049

Yang YS, Wang L (2010) Hydrological Sciences Journal-Journal des Sciences Hydrologiques Catchment-scale vulnerability assessment of groundwater pollution from diffuse sources using the DRASTIC method: a case study. Hydrol Sci Journal-Journal des Sci Hydrol 55:1206–1216. https://doi.org/10.1080/02626667.2010.508872

Zaporozec A (1981) Ground-Water pollution and its sources. GeoJournal 5:457–471. https://doi.org/10.1007/BF02484718

Zhdanov MS, Endo M, Black N, et al (2013) Electromagnetic monitoring of CO2 sequestration in deep reservoirs. First Break 31:85–92. https://doi.org/10.3997/1365-2397.31.2.66662

Zou C, Zhang G, Zhu R, et al (2013) Prediction and Evaluation Technology for Volcanic Rock. Volcan Reserv Pet Explor 151–183. https://doi.org/10.1016/B978-0-12-397163-0.00006-3